NOTICE

The quality of this microform is heavily dependent upon the quality of the original thesis submitted for microfilming. Every effort has been made to ensure the highest quality of reproduction possible.

If pages are missing, contact the university which granted the degree.

Some pages may have indistinct print especially if the original pages were typed with a poor typewriter ribbon or if the university sent us an inferior photocopy.

Reproduction in full or in part of this microform is governed by the Canadian Copyright Act, R.S.C. 1970, c. C-30, and subsequent amendments.

AVIS

La qualité de cette microforme dépend grandement de la qualité de la thèse soumise au microfilmage. Nous avons tout fait pour assurer une qualité supérieure de reproduction.

S'il manque des pages, veuillez communiquer avec l'université qui a conféré le grade.

La qualité d'impression de certaines pages peut laisser à désirer, surtout si les pages originales ont été dactylographiées à l'aide d'un ruban usé ou si l'université nous a fait parvenir une photocopie de qualité inférieure.

La reproduction, même partielle, de cette microforme est soumise à la Loi canadienne sur le droit d'auteur, SRC 1970, c. C-30, et ses amendements subséquents.

UNIVERSITY OF ALBERTA

RADIOGRAPHIC ASSESSMENT OF THE MANDIBLE AS AN INDICATOR OF SKELETAL OSTEOPENIA IN RATS

BY

C. GRACE PETRIKOWSKI, BSc, DDS, MRCD(C)

A thesis submitted to the Faculty of Graduate Studies and Research in partial fulfillment of the requirements for the degree of Master of Science.

DEPARTMENT OF APPLIED SCIENCES IN MEDICINE

Edmonton, Alberta

Fall 1991

ISBN 0-315-69954-X

Canada

UNIVERSITY OF ALBERTA

RELEASE FORM

NAME OF AUTHOR: C. Grace Petrikowski

TITLE OF THESIS: Radiographic Assessment of the Mandible as an Indicator of Skeletal Osteopenia in Rats

DEGREE: Master of Science

YEAR THIS DEGREE GRANTED: Fall, 1991

195 Wakina Drive
Edmonton, Alberta, Canada
T5T 2X5

Research is to see what everybody else has seen, and to think what nobody else has thought.

— Albert Szent-Györgyi

UNIVERSITY OF ALBERTA

FACULTY OF GRADUATE STUDIES AND RESEARCH

The undersigned certify that they have read, and recommend to the Faculty of Graduate Studies and Research for acceptance, a thesis entitled **Radiographic Assessment of the Mandible as an Indicator of Skeletal Osteopenia in Rats** submitted by C. Grace Petrikowski in partial fulfillment of the requirements for the degree of Master of Science.

Dr. T.R. Overton (Co-supervisor)

Dr. C.G. Baker (Co-supervisor)

Dr. B.A. McClean

Dr. R.E. Snyder

June 25, 1991

ABSTRACT

This study was undertaken to determine if radiographic changes in the femurs, mandibles and vertebrae of osteopenic female rats were correlated with each other and with the duration of the osteopenic state. Osteopenia was induced in the experimental groups by administering a calcium-deficient diet (CDD) to lactating (BLC; bred, low calcium) rats. Control groups consisted of virgin (VND) and bred (BND) rats fed a normal diet. Animals in each treatment group were weighed weekly and later sacrificed at fixed time intervals in the study and the mandibles, femurs and first lumbar vertebrae removed. Plain radiographs of the bone specimens were taken and the images analyzed using a computer digitizing and measuring system (CDS). The CDS was found to be precise and accurate and specimen positioning for radiography was reproducible.

The rats were uniform in weight until late in the study, at which time the BLC rats gained weight excessively, due in part to the high dextrose levels in the CDD. The CDD had no effect on pup mortality, nor did it cause any signs and symptoms of calcium deficiency in the experimental animals.

Analysis of rat femurs, vertebrae and mandibles indicated that even with long-standing calcium deficiency and accompanying skeletal osteopenia, contrary to what has been suggested in the dental literature, there were no significant changes in mandibular cortical and total widths and alveolar bone heights, nor were there any morphological changes in the first lumbar vertebrae. However, there was narrowing of cortical widths in the femurs of osteopenic animals although these changes did not progress as the animals became more severely osteopenic, suggesting that adaptation to the low-calcium state or bony equilibrium had occurred.

There were no differences in the measured variables of the femurs, vertebrae and mandibles between VND and BND animals, suggesting that pregnancy and lactation did not affect cortical widths or growth in animals fed a diet adequate in calcium. Furthermore,

even though the last group of animals was aged 48 weeks at the last measurement time, the lack of changes in cortical widths at that time compared with earlier measurements suggested that age-related changes had not yet occurred in any of the bones analyzed.

Analysis of the influence of age and weight on cortical widths indicated that generally, the age of the animals was a more significant factor than weight. Despite the excessive weight gain of the BLC group, bone parameters were not greatly affected.

It can be concluded that in the rat model of skeletal osteopenia, the mandible is not a sensitive indicator of skeletal osteopenia and other bones, such as the femur, should be used instead.

Acknowledgements

This study could not have been completed without help from the people and agencies listed below:

My deepest thanks are extended to Dr. T.R. Overton whose infinite patience, helpful criticism and sound advice during the course of the study and thesis preparation made completion of this work possible. In addition, Dr. Overton's many hours of help (beyond the call of duty) with statistical analysis of the bone measurements are greatly appreciated.

Dr. C.G. Baker for acting as a committee member and relieving me of administrative duties at the Faculty of Dentistry, allowing enough time away from other faculty responsibilities for me to complete this project. I am also grateful to the Faculty of Dentistry for the financial support given toward this study.

Drs. R.E. Snyder and B.A. McClean, who gave up valuable time from their busy schedules to act as committee members for this thesis, keenly spotting typos and other unprintables in the draft copy.

Heather Rowland, A.C.R., who not only aided in radiography of all the bone specimens, but who also became a valued and caring friend. Heather's expertise, advice and patience are deeply appreciated and were vital for successful completion of the radiography phase of this study.

Mr. Bill Andrais, A.C.R., for his help in designing and constructing the acrylic stand, his technical advice and the many philosophical discussions in his office which served not only to lower blood pressure but to plant my feet back on the ground where they belong.

The staff at Health Sciences Laboratory Animal Services in the Medical Sciences Building whose care and compassion for all animals in their facility is commendable and made my difficult work bearable.

My colleagues in the Department of Applied Sciences in Medicine for their generous moral support and their help in setting up the computer digitizing and measuring system.

My husband, Eggert Boehlau, for his patience and understanding when my research had to come first. It's your turn now.

This study was largely funded by the University of Alberta Central Research Fund.

Table of Contents

Chapter 1: Introduction and Literature Review

Chapter 2: Experimental Design and Methodology

Chapter 3: Results

List of Tables

List of Figures

List of Plates

Plate **Page**

Chapter 3

List of Abbreviations

ANOVA	analysis of variance
A-P	anterior-posterior
BLC	bred, low calcium diet
BMC	bone mineral content
BMD	bone mineral density
BND	bred, normal diet
BRU	bone remodeling unit
BSU	bone structural unit
CDD	calcium-deficient diet
CDS	computer digitizing system
CT	computed tomography
CV%	coefficient of variation
DPA	dual photon absorptiometry
HSD	honestly significant difference
IO	intermediary organization
IVNAA	in-vivo neutron activation analysis
M1	first molar
M2	second molar
M3	third molar
MI	metacarpal index
OGS	optical grid system
OVX	ovariectomy
PTH	parathyroid hormone
RMD	reversible mineral deficit
ROI	region of interest
SPA	single photon absorptiometry
TBV	trabecular bone volume
QCT	quantitative computed tomography
VND	virgin, normal diet

Chapter 1

Introduction and Literature Review

Preamble

The radiographic appearance of osteopenia in the proximal femur, vertebrae, radius and pelvis is well-documented in the clinical literature. There has, however, been very little research directed to studying the radiographic changes which occur in the jaws of subjects with documented skeletal degeneration. To the present time, the possibility of a correlation between bone mass changes in the mandible, lumbar spine and femur in either humans or animals using plain radiography has not been investigated.

This study was undertaken, using plain film radiography, to investigate the radiographic appearance of the mandible in calcium-deficient rats to determine if mandibular changes paralleled other skeletal sites in the presence of skeletal osteopenia.

Introduction

In 1986, in the United States, 247,000 women over age 45 years suffered hip fractures following minor trauma; these "bone fragility" fractures define a condition known as osteoporosis. Most of these women, however, were "osteopenic" — ie. a reduced mass of otherwise normal bone — usually over many years prior to the fracture event. Bone fragility fractures are recognized to occur in the distal radius (Colle's fracture), the vertebrae, and the proximal femur. The radial and vertebral fractures, while painful and

inconvenient for the patient, rarely result in significant disruption to the patient's life or incur any long-term disability or on-going cost to the health care system. Proximal femur fractures, on the other hand, have significant mortality and morbidity and have a great effect on patient independence and incur large on-going costs to the health care system.

Two categories of osteoporosis have been identified (Riggs & Melton, 1986): primary and secondary. Primary osteoporosis is the more common condition, and is subdivided into Type I (postmenopausal) and Type II (senile and idiopathic). Post-menopausal osteoporosis affects women 15-20 years after menopause, and is due to severe trabecular bone loss, usually manifesting as vertebral crush fractures or Colle's fracture of the distal forearm. Senile osteoporosis affects older patients where there is decreased trabecular and cortical bone as a result of aging (not linked to hormonal changes such as menopause). Idiopathic osteoporosis, however, can affect men and women of any age and results in a decrease in bone mass due to unknown etiology.

Secondary osteoporosis occurs as a direct result of an agent or disease process which causes a loss of bone mass. Examples of such etiological factors include parathyroid disease, inflammatory disorders, malignant disease, disorders of endocrine control of bone remodeling, and drugs such as corticosteroids. Often treatment of the underlying disease process results in an increase in bone mass.

Overview

In order to understand the pattern and mechanism of bone mass changes occurring in osteopenia, it is necessary to review the structural components of bone.

Cortical and trabecular bone

Structurally, there are two types of bone in the adult skeleton — cortical (compact) and trabecular (spongy or cancellous) bone. Both trabecular and cortical bone are found in every bone in the skeleton but the amount and distribution of each vary. Distinction between trabecular and cortical bone is necessary because they respond differently to external factors (eg. calcium, hormones) and differ in their radiographic appearance. Eighty percent of the skeleton by mass, is cortical bone which, macroscopically, appears solid except for microscopic spaces found within it. Although cortical bone forms the outer wall of all bones (bone cortex), the bulk of cortical bone is found in the shafts of long bones in the appendicular skeleton. Cortical bone is very low in porosity and has a low surface area:mass ratio, forming only about one-third of the total bone skeleton surface (Parfitt, 1988). Cellular and nutritional communication and bone remodeling is maintained through an interconnected canal-like network called the Haversian (or canalicular) system. From the periosteal and endosteal surfaces, Volkmann's canals (nutrient canals) enter bone at right angles to its long axis and communicate with Haversian systems. Radiographically, cortical bone appears almost uniformly radiopaque (white) and is usually fairly well-demarcated from trabecular bone.

Trabecular bone (spongiosa) has a large surface area:mass ratio (2/3 of the total skeleton surface), and is a complex three-dimensional network of curved plates and rods (trabeculae) that are continuous with the endosteal surface of the cortex, architecturally resembling the appearance of a sponge. This trabecular network encloses spaces 500 to 1000 μm in diameter which contain bone marrow ("marrow spaces"). Macroscopically, no sharp boundary can be drawn between trabecular and cortical bone and the differences between them depend only on the relative amount of solid matter and the size and number of spaces in each. Radiographically, trabecular bone appears as a radiopaque (white) lattice containing radiolucent (black) spaces. The orientation of the trabeculae is loosely described radiographically as the "bone pattern". Trabecular bone contributes only 20% of skeletal

mass and is found mainly in the axial skeleton: ribs, vertebrae, pelvis, mandible and in the ends (epiphyses) of long bones (eg. radius and femur) and is surrounded by a thin shell of cortical bone.

The external surface of every bone, except over the articular surfaces, is covered by a specialized fibrous connective tissue cover — the periosteum. Periosteum consists of two tissue layers which are not sharply defined. The outer layer is dense fibrous tissue containing a network of thin-walled blood vessels and the inner layer is loose connective tissue which, in adults, contains osteoprogenitor cells. The new bone formed by periosteum in some neoplastic and reactive conditions is formed by apposition and may be termed "periosteal new bone". (Leeson and Leeson, 1981)

Osteopenia

Osteopenia, defined as a decrease in bone mass of otherwise normal bone tissue, must be distinguished from osteoporosis, defined as a decrease in bone mass such that fracture occurs with little or no trauma. Although osteopenia can result from several systemic diseases, drug effects or exogenous factors, the emphasis in this work is its relationship to osteoporosis.

In order to assess osteopenia, a variety of bone mass measurement techniques are available and these will be discussed in more detail later. Generally, bone mass is measured in particular bones (eg. distal radius or proximal femur) and this information then used to estimate total bone mass.

At present, bone mass measurements are not done routinely in clinical practice; only patients at risk for osteopenia undergo these procedures. Consequently, a significant portion of the population does not benefit from early diagnosis of decreased bone mass. However, a large percentage of the population undergoes routine x-ray procedures, particularly dental x-rays, on an annual or semi-annual basis. Theoretically, osteopenia could be detected in dental radiographs. Affected patients who otherwise would not have

been screened for osteopenia by other methods could therefore be identified and referred for comprehensive evaluation and management. This is the context of the present study where the radiographic appearance of the mandible, first lumbar vertebra and femur are compared in osteopenic rats.

Background and Literature Review

Bone biology

In order to understand the physiological mechanisms underlying osteopenia, a basic understanding of bone biology is prerequisite. Frost (1982) conceptually described the biological organization of man in terms of a ladder, with each rung (or level) possessing distinct biological properties. In Frost's model, the lowest rung represents the cellular level, the middle rung the tissue level, and the top rung the organ level. The tissue level, acting as a bridge between the cellular and organ levels, is termed the intermediary organization (IO) and also serves to control the entire system. These concepts can be depicted as shown in Fig. 1.1.

The tissue level of organization is further subdivided into three levels; the upper, middle and lower intermediary organization levels. The upper IO level represents the envelope system, consisting of four anatomically distinct bone surfaces which also have distinctive bone balances and bone turnover. The four bone envelopes include: (1) periosteal surface or envelope which gains bone throughout life; (2) trabecular envelope which loses bone; (3) cortical-endosteal envelope which also loses bone, and (4) Haversian envelope which remains relatively stable throughout life. The middle IO level consists of remodeling, modeling, growth and other functional entities such as homeostasis and repair. The lower IO level defines the state of cellular activities and relationships underlying the functional units of higher IO entities.

Fig. 1.1 The biological organization of bone. (Frost)

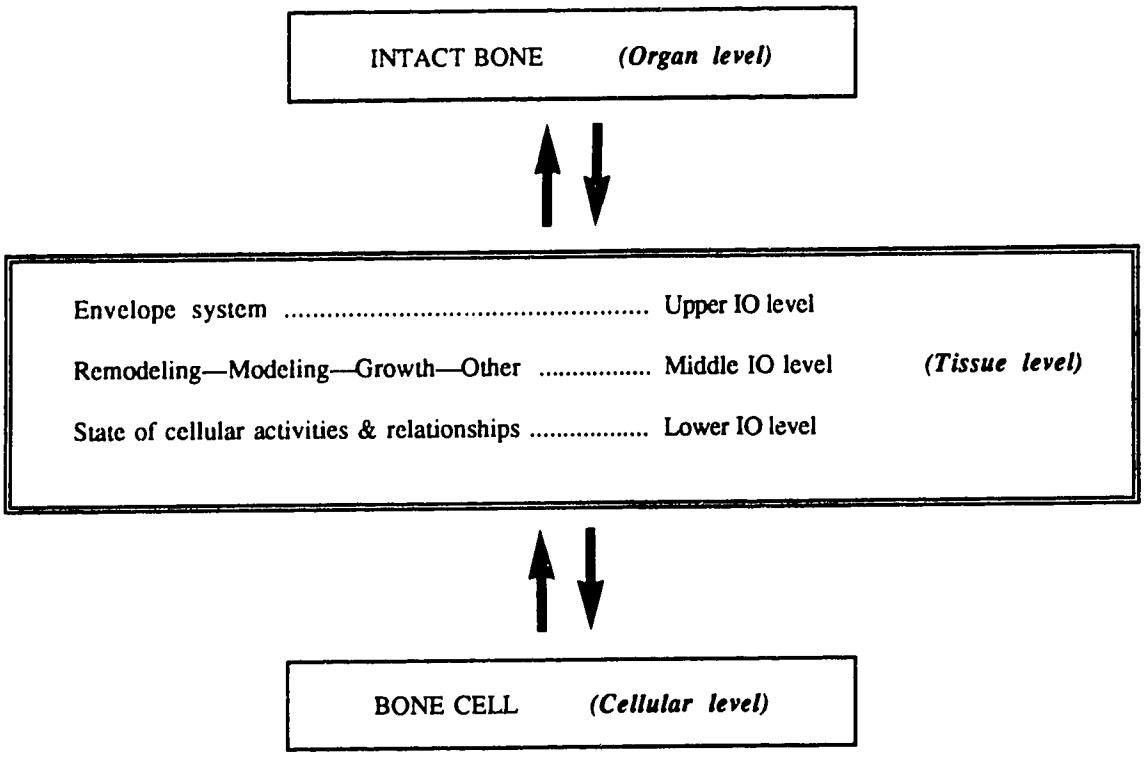

Bone

The bones of the skeleton are metabolically active and able to adapt to the varying mechanical and metabolic demands placed upon them. Apart from their function in providing locomotion, protection of vital organs, and support and strength to the body, the skeleton acts as a mineral reservoir of calcium and phosphate. Depending upon the levels of serum calcium and phosphate, bones may be required to release (or store) these minerals according to metabolic needs; in addition, mature bone undergoes continuous cycles of bone remodeling, which will be discussed later.

Bone is made up of connective tissue consisting of cells and an intercellular matrix. The matrix contains both an organic component called osteoid, consisting chiefly of collagen and noncollagenous proteins, and an inorganic component which accounts for 70% of the weight of bone. The inorganic component is responsible for the hardness and rigidity of bone and is made up of a mineralized substance (hydroxyapatite) which is principally calcium and phosphorus. Other ions found in the mineral component include carbonate, magnesium, sodium and fluoride. Also found in bone are collagenous fibers which contribute to the strength and resilience of bone.

The principal cells of bone are osteoblasts and osteoclasts, and these will be described in more detail later. Osteoblasts are involved in bone formation, and osteoclasts in bone resorption. The actions of these two cell types are linked through a coupling mechanism which ensures that osteoblasts appear at sites excavated by osteoclasts.

Bone compartments and bone modeling

Macroscopically, bone exists in one of three states at any given time: (1) "old bone" which is fully mineralized and inactive; (2) "mineralizing space" which is new bone in the process of being mineralized; or (3) "remodeling space" which refers to the temporary absence of bone following the resorption phase of the remodeling cycle (Fig 1.2). The proportion of skeletal mass in each of these states varies depending on the individual's genotype, physical status and lifestyle, and the proportions can respond quickly to change.

Bone modeling occurs during skeletal growth and refers to the change in size and shape of bones during each developmental stage both pre- and postnatally. Modeling is complete at skeletal maturity after which only remodeling of bone occurs.

Fig. 1.2 Hypothetical bone compartments in the skeleton

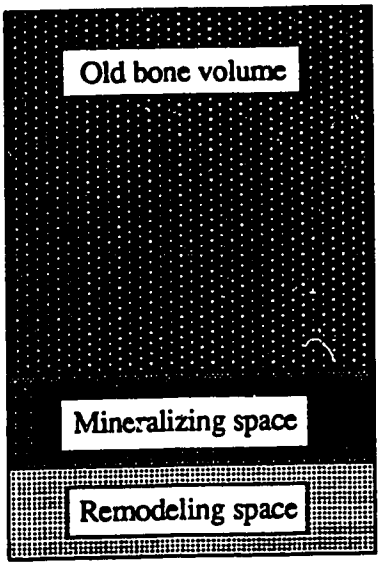

Bone remodeling

Bone remodeling is the mechanism for bone replacement in the adult skeleton which maintains biomechanical competence of the skeleton by preventing the accumulation of fatigue damage and maintaining an adequate supply of young bone of relatively low mineral density to subserve mineral homeostasis. Remodeling is a semi-microscopic tissue turnover or replacement which can occur without altering the gross architecture or size of the affected structures (Frost 1982). Osteoblasts and osteoclasts work together to continuously remove and replace volumes of bone tissue in order to prevent bone fragility and eventual fracture. In distinguishing modeling from remodeling, growth determines the size, modeling determines the shape and remodeling then maintains functional competence of bone.

Bone remodeling can be activated or inhibited by various systemic and local factors. Putative activators of bone resorption include parathyroid hormone, prostaglandins,

vitamin D, thyroid hormone, and interleukin 1. On the other hand, interferon, calcitonin, estrogens and bisphosphonates are putative inhibitors of bone resorption.

Remodeling activity occurs at all four bone surfaces: (1) periosteal; (2) intracortical (including both Haversian and Volkmann canals); (3) endocortical (endosteal); and (4) trabecular, with the latter three surfaces being in continuity (Parfitt, 1988). Important metabolic exchange occurs mainly on the internal bone surfaces; the periosteal surface is relatively quiescent in healthy subjects.

Bone remodeling occurs as a sequence of discrete cellular events in a theoretical entity called a bone remodeling unit (BRU). A completed remodeling sequence results in a new physical quantity of bone called a bone structural unit (BSU). The skeleton consists of many small pieces, each of these pieces consisting of a BSU. In the average skeleton, there are approximately 35 million BSU's with an average volume of about 0.05 mm^3 (Parfitt, 1981). Parfitt likens remodeling to laying down the bricks of a building; it is performed in temporally and spatially discrete episodes with each brick representing a BSU. The BSU's are held together by a highly mineralized but collagen-poor connective tissue (analagous to bricks held together by mortar), microscopically visible as a cement line. Accordingly, if bone is viewed under a high powered microscope, it has the appearance of building bricks rather than a piece of poured concrete (Parfitt 1981). The cement lines either represent reversal lines, which mark the furthest extent of a previous episode of bone resorption, or they represent arrest lines, indicating that the BSU was completed in two or more separate periods rather than continuously.

Remodeling has six distinct stages and is illustrated in Fig. 1.3 (Parfitt):

1. Quiescence

At any one time, 80-95% of bone is inactive and does not participate remodeling, ie. it is in a state of quiescence. The bone surface is covered by a thin layer of bone lining cells that arise by terminal transformation of osteoblasts. These cells are postulated to retain the ability to function as osteogenic precursor cells.

2. Activation

Activation starts the process of remodeling and is said to occur when a small area of quiescence begins remodeling activity. This stage begins with recruitment of osteoclasts which subsequently gain access to the bone surface. Activation occurs when remodeling stimuli (eg. hormones, physical forces, microdamage) locally alter the behavior of the lining cells, and thereby expose underlying bone surfaces that contain chemical attractants for the osteoclasts.

3. Resorption

Once in contact with bone, osteoclasts erode a cavity in bone (with an average volume of 1/10 mm^3) by release of hydrolytic enzymes. The bone cavity is termed a Howship's lacuna in trabecular bone and a cutting cone in cortical bone.

4. Reversal

The reversal stage is an intermediate stage between completion of resorption and commencement of formation at a particular BRU and lasts one to two weeks. Histologically, the Howship's lacuna is devoid of osteoclasts during this time but contains mononuclear cells (reversal cells). Some of the reversal cells partly smooth over the ragged surface left by the resorptive process and deposit a thin layer of cement substance, preparing the surface for bone formation. The cement substance consists of a highly-mineralized but collagen-poor connective tissue, visible as a "cement line" in two-dimensional histologic sections. Most cement lines represent reversal lines which have a scalloped appearance, are stained by acid phosphatase, and have discontinuous canaliculae and abrupt changes in lamellar orientation. Other cement lines represent arrest lines which have a smooth surface, lack of acid phosphatase staining and continuity of canaliculae and lamellar orientation.

5. Formation

Bone formation occurs in two stages: matrix synthesis followed by mineralization, which are separated in time and space. Soon after completion of the cement line, osteoblasts appear and refill the cavity with bone matrix (osteoid). Osteoblasts trapped within the newly-formed matrix become osteocytes. The osteoid begins to mineralize after 5 to 10 days of maturation with the entire formation stage normally spanning a period of 3-4 months in man. After primary mineralization is complete, the osteoid seam disappears. With complete mineralization, (after about 2 years in healthy subjects) the cells remaining on the surface transform back into flat lining cells.

6. Quiescence

Upon termination of the remodeling cycle, the new BSU is completed and the surface returns to a quiescent state.

The time required for each BRU to complete the remodeling stages from resorption to formation (sigma, σ), is 3-4 months in cortical bone and 2-3 months in trabecular bone in the young, healthy skeleton. Mineralization requires a longer time period to complete; 80% of "old" bone density is attained after about 2-3 months ("primary mineralization") but up to 2 years is necessary to achieve 100% mineralization ("secondary mineralization"). The reason for this long time span is that hydroxyapatite, like osteoid, requires a period of maturation which involves changes in the structural and chemical nature of the mineral.

Fig. 1.3. Normal bone remodeling of a single BRU and construction of a single new BSU.

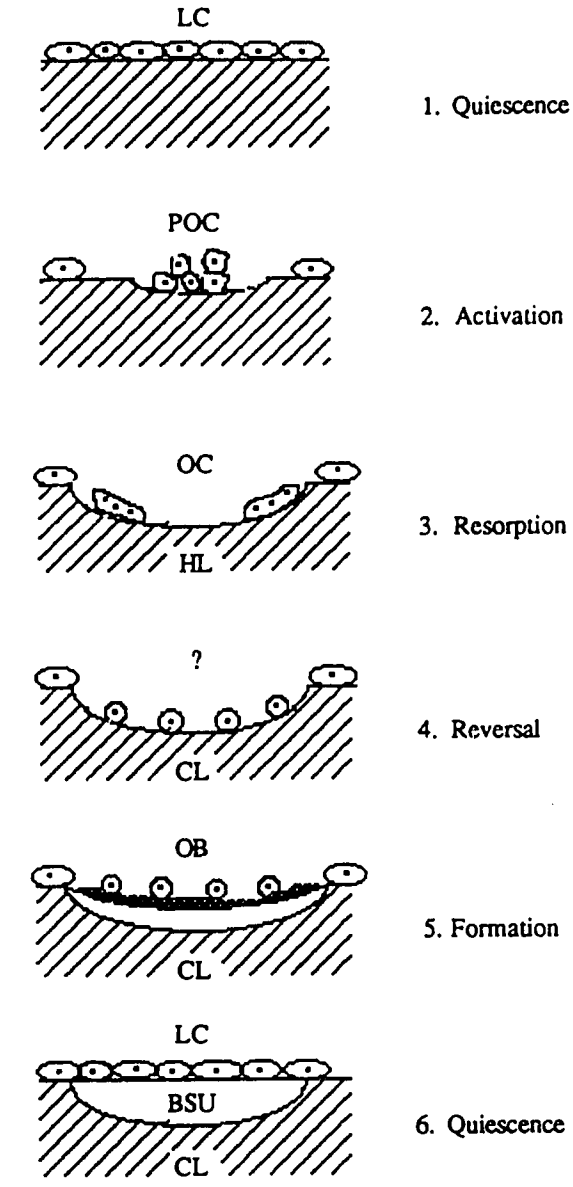

LC - lining cells
POC - pre-osteoclasts
OC - osteoclasts
? - unknown cell type
HL - Howship's lacuna
CL - cement line (reversal line)
OB - osteoblasts
BSU - bone structural unit

Bone turnover

"Bone turnover" is a broad term describing the cumulative effects of bone remodeling. According to Parfitt (1988), the whole-body rate of bone turnover at the organ level is about 10% per year; 4% in cortical bone and 25% in trabecular bone. The rate of bone turnover at the tissue level only depends on the net bone balance at the BRU level whereas the organ level of bone turnover also depends on the activation frequency (ie. the number of BRU's initiated per unit time). With activation, many BRU's are recruited simultaneously and the local bone density initially decreases as "coherent" resorption proceeds. Conceptually, when the BRU precursor "pool" is full, the potential for further activation is high and when the BRU precursor pool is empty, the potential for further activation is low.

Bone cells

Several different bone cell types are important in bone modeling and remodeling. The cell responsible for bone formation is the osteoblast. Osteoblasts form a continuous sheet of cells which, in their active state, are cuboidal, asymmetric, and contain intracellular organelles typical of cells vigorously engaged in protein synthesis. These cells are oriented according to underlying bone matrix fibers. Resting bone surfaces are lined by flattened cells that are believed to be inactive osteoblasts, also called bone lining cells (Peck and Woods, 1988). Histologists describe this appearance as "osteoblastic rimming". In addition to collagen, osteoblasts synthesize various matrix components, including osteocalcin, osteonectin and inductive factors as well as other substances. Osteocalcin is a chemotactically-active bone matrix protein that contains three γ-carboxyglutamic acid residues which allow it to bind to bone. Osteocalcin is postulated to act in preventing excess mineralization of bone. Osteonectin, on the other hand, is a phosphoserine-containing glycoprotein which binds to collagen and hydroxyapatite, forming a complex

which potentiates calcium-phosphate deposition. Osteonectin is probably involved in hydroxyapatite nucleation, stabilization, and organization.

As osteoblasts become incorporated into the matrix they synthesize, osteocyte lacunae are formed by deposition of collagen fibrils which later mineralize. At this point, the osteoblasts "convert" into osteocytes which function in perilacunar bone resorption and bone formation. Osteocytes function together with bone-lining cells to play a role in calcium flux between intraskeletal lacunae and bone surfaces to the extracellular fluids. In addition, osteocytes have the ability to become osteoblast-like in nature, synthesizing matrix proteins in order to repair microfractures (microscopic localized bone fractures due to everyday bony stresses) and resorption-mediated defects resulting from bone remodeling. They may also be involved in stabilization of bone mineral by maintaining an appropriate local ionic milieu.

Bone resorption is accomplished mainly by osteoclasts. These large, multinucleated cells attach to bone surfaces by a special attachment region which characteristically has a ruffled border surrounded by an organelle-free, actin-containing clear zone. The ruffled border is the site of active bone resorption; osteoclasts which are mobile and not actively involved in bone resorption do not have a ruffled border. Osteoclasts are derived from a stem cell found in hematopoietic tissue and later form by fusion of several cells, accounting for their multinucleated appearance. Mature osteoclasts migrate to bone surfaces where they initiate bone resorption. The actions of osteoblasts and osteoclasts are linked through a coupling mechanism which ensures that osteoblasts promptly appear at sites excavated by osteclasts. There must be an adequate supply of new osteoblasts at the right place at the right time and each new osteoblast must be able to make a normal amount of bone matrix, a process which is probably unrelated to coupling (Parfitt 1982).

Other important bone cells include mast cells, monocytes, macrophages and lymphoid cells. Mast cells participate in the regulation of remodeling whereas monocytes

and macrophages modify tissue development, organization, remodeling and repair. Lymphoid cells influence the development and activity of bone cells.

Bone density

Evaluation of skeletal osteopenia requires some estimation of bone mass. Various methods of measuring bone density (discussed later) are available to the clinician and depending upon the method used, the term "bone density" may have several different meanings. In plain film radiography, the terms "bone density" and "optical density" are often used interchangeably to define the amount of film blackening (radiographic density) seen in the spongiosa of the image. That is, if the overall radiographic image is very dark (black or "dense") despite proper film exposure and development, the patient is described as osteopenic. On the other hand, measurement of bone density by quantitative computed tomography (QCT) refers to average physical density of a well-defined volume of bone tissue, rather than radiographic density. These are important distinctions and must be clarified when discussing bone mineral content. With the onset of skeletal osteopenia, bone density, regardless of its definition, decreases. Osteopenic bone is normal in every way except that there is simply less bone present in a given volume. This should be contrasted with osteomalacia where bone is not mineralized properly and exhibits large amounts of unmineralized osteoid. In both cases, bone density has decreased but the underlying mechanisms differ.

As stated earlier, trabecular bone has about a 10X higher turnover rate than cortical bone, principally because of its high surface-to-volume ratio, which makes it a sensitive parameter for monitoring diseases affecting bone (Genant, 1985). For this reason, trabecular and cortical bone should be considered separately when comparing data for total bone density (cortical and trabecular bone) with data for cortical bone alone, such as the metacarpal bone index (Fig. 1.4). Trabecular bone density in the peripheral skeleton is a fairly reliable index of postmenopausal osteoporosis, and trabecular bone should react

similarly throughout the skeleton in the presence of generalized bone disease (Ruegsegger 1984).

Fig. 1.4 Metacarpal bone index used for estimating bone density.

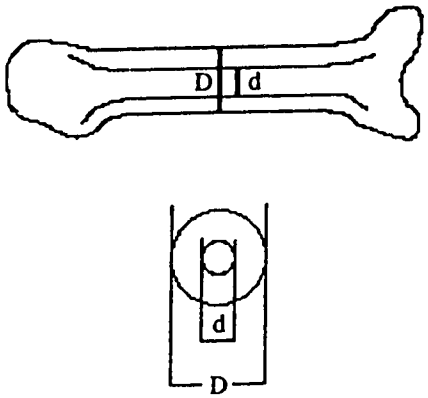

Cross-section of metacarpal

The sum of the total width (D) and trabecular width (d) at the midpoint of the first metacarpal are divided by the total width to yield the metacarpal index measurement.

Methods of bone mass measurement

Bone mass measurements are useful diagnostic procedures for identifying patients at risk for skeletal osteopenia as well as for assessing the progress of disease and therapy in those patients already diagnosed with skeletal diseases. Several methods are available for bone mass quantification; the choice of which to use depends on several factors including availability and cost of equipment, radiation dose (especially if several follow-up examinations are necessary), sensitivity to changes in bone mass and the precision and accuracy of the technique. Precision is the reproducibility of the measurement technique and reflects variations between independent measurements of the same quantity of bone. Accuracy is the ability to measure the absolute amount of bone present and is a true representation of the quantity of bone tissue in a measured volume. Sensitivity is defined

in terms of measured changes in bone mass relative to real changes in bone quantity in the measured volume. Therefore, an ideal bone mass measuring method has high precision (ideally better than 1%) as well as high accuracy and sensitivity so that small changes in bone mass over time can be documented.

Other factors influencing the choice of measurement technique include the type of bone (cortical vs. trabecular bone) and measurement site (eg. radius, vertebrae, proximal femur). Most metabolic bone diseases are detected earlier in trabecular bone and affect it to a greater extent than cortical bone due to the higher surface to volume (mass) ratio of trabecular bone. Sites containing large amounts of trabecular bone include the distal radius, proximal and distal femur and the vertebral bodies. In the past, the appendicular skeleton was used for bone mass measurements because of accessibility and ease of measurement with good precision but modern techniques use the lumbar vertebral bodies for bone mass assessment. Various methods of bone mass measurements are outlined in the following sections.

Plain radiographs - Radiogrametry

Radiogrametry is the simplest of the quantitative radiological techniques to assess the skeleton; it involves a measurement of the cortical thickness or another parameter at a predetermined site of bone in plain radiographs using a micrometer or similar measuring instrument. The results are normalized to bone width to compensate for variations in body size. In osteopenia, increased cortical-endosteal resorption usually results in reduced cortical thickness in the appendicular skeleton. By measuring cortical thickness, an estimation of overall bone mass can be made. Unfortunately, a 30-60% change in the mineral content in bone must occur before it is detectable in a plain film radiograph and for this reason, radiogrametry is not the technique of choice for early detection of skeletal osteopenia.

Several sources of technique error are possible using radiogrametry: error in positioning the bone before the radiograph is exposed, error in machine alignment, inaccurate measurements due to edge gradient in the radiographic image, and other observer error, both in measurement technique and in choosing a reproducible area of the part to be measured, especially if several subjects are compared.

Using plain radiographs, several parameters can be measured: width of cortices and medullary spaces, cross-sectional area of bone, wedge angles of compressed vertebrae, and overall shape and size of bones. Linear measurements can be made using a combination of calipers and a magnifying glass, a micrometer, or by using a computerized digitizing and measuring system. Rico and Hernandez (1989) compared the accuracy of using calipers with and without a magnifying glass to determine the metacarpal index in a series of hand radiographs. They concluded that such measurements should ideally be made by the same observer and that use of a magnifying glass increased measurement accuracy and decreased interobserver variability.

Virtama and Helelä (1969) studied radiographic measurement of cortical bone, measuring the thickness of the cortical layer of the long bones to determine normal values. They concluded that the best parameter for estimating mineral content of long bones from plain radiographs was combined cortical thickness, defined as the sum of both cortical layers at the same level measured in one direction. Because cortical thickness was only measured at one point, local disturbing factors could affect the results. The authors cautioned that for this reason, no single measurement could be very dependable and that measurements of several bones from the same subject may have given more information. If abnormal results were obtained from more than one bone, a pathological condition was likely present. In addition, due to mechanical forces, gravitational weight-bearing bones such as the femur were less suited for cortical bone measurements than the metacarpals or radius. Non-gravitational weightbearing bones, presumably including the mandible, were the most stable, especially in active subjects.

Visual estimations of the degree of bone mineralization in radiographs (bone "density") are commonly made in clinical situations. The accuracy of this practice has been studied by Finsen and Anda (1988) and found to be poor; no significant difference in the rate of correct identification of osteopenia in metaphyseal and diaphyseal bone was observed between three observers but the probability of correctly identifying osteopenic changes in radiographs increased with increasing severity of actual bone mineral density differences. Based on these findings, it is inadvisable to visually estimate bone density from plain radiographs.

Intra- and inter-observer variability is another potential source of error in bone mass measurements. Naor et al. (1972) studied intra-observer variability in measuring the metacarpal index and outlined the following sources of variation in metacarpal measurements:

1. Measurement variation - due to inherent limitations of the measuring instrument used.
2. Observer variation - the inherent variability in the observer's siting of the film and the eyepiece, fatigue, etc.
3. Location error - determination of the mid-shaft line and exact location to be measured.

In order to reduce measurement variability, two measurements of the cortical index were taken and averaged for the final result. In addition, paired measurements which differed significantly from each other were excluded from the analysis. The authors concluded that over time, an observer may improve his degree of reproducibility, particularly if cortical index assessments on a group of films are carried out within a short period of time, in order to aid in preserving adherence to the original measurement criteria. In addition, measurements were more accurate if the films were of good diagnostic quality.

Adams et al. (1969) also studied observer error in metacarpal measurement and found that there were large intra- and inter-observer errors in the measurements,

particularly for the measurement of cortical thickness; the degree of error increased if the measurements were taken at widely separated time intervals. The authors concluded that in comparative studies, radiographs must be measured in random order and that the measurements should be done in a short time frame. Bland et al. (1969) had similar findings and also noted that knowledge of the diagnosis of osteopenia influenced the observers. In addition, radiography of the subject's bone along with a standard (cadaver bone) made no significant difference in the detection of osteopenia in the bones of the subject, again emphasizing that visual estimations of bone density are unreliable.

Photodensitometry

Photodensitometry is measurement of radiographic density, that is, a quantitative evaluation of the various grey levels in a radiograph. A normal radiograph of a body part is taken with carefully standardized exposure factors, development and patient positioning. An aluminum stepwedge is simultaneously exposed on the same film for density calibration. Soft tissue equivalent material above and below the body part, such as a water bath, is often used to improve accuracy of the technique. Optical density readings are obtained and referenced to the stepwedge to provide values (projection points) reflecting the amount of bone in the beam path. The projection points obtained along a line across the bone form a projection curve which is then used to determine the total amount of bone in the measured cross section. Bone mineral content is then expressed in units of grams per centimeter (g/cm).

The radiation dose to the subject is the same as for a normal radiograph. Precision of the technique is reported as ±4.7% for the metacarpal and ±8% for the ulna (Shimmins et al., 1972; Cameron et al., 1963). Since cortical bone mass is also included in the measurements, this technique has limited uses because small changes in the trabecular bone mass cannot be detected with adequate precision.

Single photon absorptiometry (SPA)

SPA was introduced by Cameron and Sorensen in 1963 and was the first technique available to quantitatively determine bone mineral density. A radioactive source, usually ^{125}I (average energy = 28 keV) or ^{241}Am (energy = 60 keV), emits photons which are collimated into a narrow beam which passes through the subject to a photon detector. The detector measures the intensity of the transmitted beam and hence the attenuation of the emitted beam caused by the subject. The relative attenuation is proportional to the bone mineral content (BMC) and results are usually expressed in g/cm. In order to compensate for soft tissue thickness, the limb scanned is usually immersed in a water bath. The source and detector are mechanically rigid and move linearly across a limb in a single pass or are moved in a rectilinear manner to cover a larger area.

The precision of SPA depends upon the bone site chosen (usually the radius) and upon repositioning in repeated measurements. For the distal radius, precision varies from ±1.4% to ±7.6% (Hangartner, 1986) because of difficulty in accurate repositioning of the forearm in longitudinal studies. According to Cameron (1968), the accuracy of SPA is 5-6% and is affected by variations in the amount of fat present in the bone marrow. This technique is easy to use, inexpensive and delivers a very low local radiation dose to the patient (0.02 mSv) (Hangartner, 1986). However, the technique has several disadvantages. Because of the requirement for a constant tissue thickness across the scan path, the technique is limited to appendicular skeleton sites such as the ulna, radius and os calcis. These sites are now known to be not as diagnostically useful as the spine and femur for detection of osteopenia in the axial skeleton. In addition, SPA has low sensitivity because it measures total bone mass at sites where cortical bone predominates. Since osteopenia affects trabecular bone before cortical bone, SPA has limited value for early detection in osteopenic subjects.

Dual photon absorptiometry (DPA)

DPA is similar to SPA except that it uses two photon energies instead of one, allowing measurement of bones which are not accessible by SPA, particularly the spine and femur. Because photons of two different energies are emitted by the isotope, the need for constant thickness and homogenous soft tissue cover around the bone are eliminated. ^{153}Gd (44 keV, 100 keV) or a combination of ^{125}I with ^{241}Am (29 keV and 60 keV respectively) are often used. Bone density is reported in g/cm^2, reflecting the fact that the bone mass (grams) is divided by the area (cm^2) of the bone scanned. Precision is approximately 2% for the lumbar spine (Mazess and Barden, 1989) and accuracy is approximately 4% (Peppler and Mazess, 1981; Hangartner, 1986). The radiation dose is 0.01 to 0.05 mSv. Although DPA allows BMC measurement for the entire skeleton, it does not differentiate between trabecular and cortical bone, limiting its usefulness in detection of early skeletal osteopenia.

Dual energy radiographic densitometry (DER) or dual energy x-ray absorptiometry (DEXA)

These terms refer to the same DPA technique but an x-ray tube is used instead of a radioactive isotope to generate photons at two energies, usually 40 and 70 keV. According to Mazess and Barden (1989), the higher radiation flux achievable using x-ray sources provides several advantages over conventional DPA including improved spatial resolution, improved precision (1 vs 2%) and greatly decreased scan times. The main disadvantage of this technique, as with SPA and DPA, is that it cannot distinguish between cortical and trabecular bone.

Quantitative computed tomography (QCT)

Computed tomography (CT) can also be used to measure the photon attenuation caused by an object. In diagnostic radiology, CT is used for imaging body parts,

providing an alternative or adjunct to plain film imaging. However, because attenuation is measured, this information can also be used to determine BMC. With advancing technology, CT scanners have been improved in design and efficiency but the basic principles of their operation have remained the same. Current systems consist of a radiation source which emits a highly-collimated photon beam (x- or γ-rays) which pass through the subject. Collimated detectors, rigidly connected to the source, measure numbers of transmitted photons as the source-detector assembly rotates repeatedly through small angles about the subject, each time obtaining an attenuation profile (set of data).

Through mathematical reconstruction from the attenuation profiles, a two-dimensional map of the x-ray attenuation coefficients in a cross-section of bone is produced, and these coefficients can be used to determine tissue density at any point in the image. A bone equivalent (such as K_2HPO_4) reference standard ("phantom") is usually required for calibration and the determination of bone mineral density (BMD) using commercial scanners. Bone density is expressed as K_2HPO_4 equivalent (mg). Using CT methods, cortical, trabecular or total BMD can be measured.

Two types of quantitative CT are available: one is a special-purpose CT scanner (γ-CT) for measurements in the appendicular skeleton (eg. distal radius); the other is a commercial whole-body CT scanner system with a calibration phantom that is measured simultaneously with the patient (Hangartner, 1986). The γ-CT scanner has a precision of better than ±1.0% for in long-term clinical studies of trabecular bone density in the distal radius (Overton, 1987) and an accuracy of -0.6 to +3.4% (Hangartner et al., 1987). A low keV photon source (^{125}I, 29 keV) is used and skin dose is low — 0.15 mSv per scan. Errors in bone density measurements due to marrow fat are small because the low photon energy provides a high contrast between bone and soft tissue. Such scanners are useful in longitudinal studies, and they have the ability to measure trabecular bone without including cortical bone. However, these scanners have limitations, most important of which is that they can only measure appendicular sites.

Commercial whole-body scanners generate cross-sectional images of selected vertebrae using x-rays rather than γ-ray photons; both single and dual-energy scanners have been developed. The patient and calibration phantom are scanned together and a region of interest (ROI) defined in the resulting bone image. The average pixel value of the ROI is compared with that of the phantom, yielding bone density in terms of densities of standard solutions. Advantages of this technique include the ability to measure the predominantly trabecular core of the vertebral body and/or the entire vertebral body. However, the precision of bone mass measurement is relatively poor (±1.7%) because bone occupies only a small area of the image. Accuracy is also poor and varies between -2.7 and +7.3% (Hangartner et al. 1987). Sensitivity to changes in bone density is also low due to the relatively high (140 kVp) x-ray tube potential (Müller et al., 1985). The radiation dose for scans made with commercial systems is fairly high (about 2.5 mSv), about 20 times higher than for SPA, DPA and γ-CT .

In-vivo neutron activation analysis (IVNAA)

Using in-vivo neutron activation analysis (IVNAA), neutrons irradiate either small body areas or the entire body. Neutrons are generated by nuclear reactors, nuclear accelerators or are emitted from radioisotope sources such as ^{238}Pu-Be, ^{241}Am-Be, ^{252}Cf. Neutron irradiation of stable calcium (^{48}Ca) in the body converts some of it to a radioactive form (^{49}Ca), which then emits γ-ray photons at an energy of 3.1 MeV. Scintillation detectors are used to count these γ-rays; the number of γ-rays per unit time are equated via a calibration procedure to the total amount of calcium in the body volume irradiated.

Depending on body size, the precision of IVNAA is between ±2% to ±7%. The radiation dose is about 50 mSv if a localized area, such as the hand, is examined (Catto et al., 1973; Hangartner, 1986). The accuracy of this method is poor in patients with extraskeletal calcifications, limiting its usefulness in diseases manifesting dystrophic

calcification. Because of these limitations, IVNAA is not routinely used for calcium determination in humans.

Human studies

Much interest has been focussed on early detection and treatment of skeletal osteopenia and osteoporosis in humans. Studies correlating BMC of the femur, first metacarpal and one or more lumbar vertebrae have been undertaken in the past. More recently, studies correlating BMC changes in these bones with changes in the mandible have been reported, reflecting the dental profession's interest in skeletal osteopenia, and are described in further detail below. This section will focus on studies of bone mass changes in the femur, spine and first metacarpal, and the relationship between the mandible and these other skeletal sites.

Trabecular pattern, bone structure and osteopenia

The trabecular pattern (trabecular arrangement) of bone is reported to indicate an alteration in bone density and bone disease. Singh (1970) suggested that trabecular arrangement in the neck of the femur might indicate which patients were at risk for vertebral fracture (and osteoporosis). However, Singh's interpretations were later found to be only partially correct since the femoral neck trabecular arrangement reflects age-related changes in the biomechanical forces in the hip rather than the presence of osteopenia per se. With age, hip musculature becomes flaccid, allowing the femoral head to migrate out of the acetabulum resulting in changes in femoral neck angle of adaptation. The trabecular pattern adapts to these altered biomechanical forces, emphasizing that trabecular arrangement is not only an indicator of skeletal osteopenia, but also of biomechanical function of the structure.

Pødenphant et al. (1987) examined the amount and structure of mineralized bone in postmenopausal women with and without vertebral compression fractures. The vertebral

compression group had predominantly trabecular bone loss, seen in plain x-rays, and deteriorated trabecular microstructure, seen with histomorphometry. Loss of cortical bone was also noted in these patients. According to Ruegsegger et al. (1984), trabecular bone loss in postmenopausal osteoporotic patients shows a step-wise pattern in which phases of relative stability are followed by brief phases of rapid bone loss. Assuming that this phenomenon also occurs in other osteopenic diseases, caution must be used in interpreting data gathered at widely separated points in time because the rapid bone loss phase or conversely, the stable phase, may not be represented in the data.

The biomechanical competence of trabecular bone is dependent not only on the absolute amount of bone present but also on the trabecular microstructure. Kleerekoper et al. (1985) found that patients with vertebral compression fractures due to postmenopausal osteoporosis had a lower mean trabecular plate density and a lower number and connectivity of structural elements in the iliac crest. However, these findings cannot be extrapolated to the mandible because its trabecular pattern is too variable to act as a reliable indicator of skeletal osteopenia.

Parfitt (1984) studied age-related structural changes in trabecular and cortical bone and proposed two structurally different forms of bone loss with different rates, cellular mechanisms and biomechanical effects. He divided age-related bone loss into two categories: (1) rapid and (2) slow bone loss. Rapid bone loss results from excessively deep osteoclastic resorption cavities leading to perforation of structural elements, increased size of marrow cavities and discontinuity of bone structure in trabecular bone. In cortical bone, rapid bone loss results in subendosteal cavitation and conversion of the inner third of the cortex to a structure similar to trabeculae which then undergoes similar changes to those occurring in trabecular bone. The result of these structural changes is that bone strength is significantly reduced. On the other hand, slower bone loss involves incomplete refilling of resorption cavities by osteoclasts, resulting in new bone layers which are too shallow. This leads to thinning of residual structural elements in both trabecular and cortical bone,

histologically seen as a reduction in mean wall thickness. Bone strength is reduced in proportion to reduction in the amount of bone, in contrast to rapid bone loss where bone strength is reduced to a greater extent than reduction in the amount of bone alone would suggest. During this period of endosteal bone loss, compensatory localized trabecular thickening may occur in some areas, such as the vertical trabecular plates in the spine and other areas which may be subjected to compressive forces.

At the same time that endosteal bone is lost, bone is slowly added to the periosteal surface by slight overfilling of resorption cavities. Parfitt cautions that although the periosteal gain partly offsets the structural weakness resulting from endosteal loss, it is not directly compensatory. This mechanism of periosteal bone formation is present and active (to a limited extent) throughout life, probably in order to respond to the need for fracture healing or to increased biomechanical demand and is not necessarily a consequence of endosteal bone loss.

Metacarpal index (MI)

The metacarpal index (MI) has been shown to be a useful parameter in the assessment of osteopenia (Pogrund et al. 1979, 1981). Since skeletal osteopenia will also manifest in the metacarpals, measurement of metacarpal cortices provides a good estimate of metacarpal and presumably, also overall skeletal bone mass. In this index, the percent ratio of the cortical thickness of the second metacarpal at its midpoint is compared to the total width of the metacarpal (Fig. 1.4). Pogrund found that if osteopenic changes were detected in the hand, osteopenic changes in the spine were also present. However, the *absence* of osteopenic changes in the hand does not rule out the possibility of osteopenic changes in the spine, and presumably, other skeletal sites.

Metacarpal index-mandible correlation

Von Wowern and Stoltze (1979b) compared the MI to changes in cortical mass and cortical width at a standard site of the mandible. They found that the MI was significantly related to the percentage changes in bone mass and in mean cortical width in the buccal cortex at a standard site of the mandible. Accordingly, the MI should be useful in providing a rough estimate of the changes in the mandible in longitudinal studies if baseline values were first obtained for each individual.

In comparing the osteopenic changes in the metacarpals with alveolar bone resorption, Ward et al. (1977) found no correlation. The amount of alveolar bone loss in edentulous patients is related to many factors in addition to skeletal osteopenia so the MI is not a useful predictive index.

From these studies, it appears that the MI is more useful for predicting mandibular bone mass rather than the degree of edentulous ridge resorption.

Mandibular bone density and bone mineral content (BMC)

Relatively few studies have investigated osteopenia in the human mandible. Methods for measuring mandibular "bone density" and "bone mineral content" in osteoporotic patients have been reported by Kribbs et al. (1983a&b; 1989), Henrikson et al. (1974a&b) and von Wowern (1985) but these previous studies did not evaluate the changes seen in plain films.

Kribbs et al. (1983) studied osteoporotic females to determine the relationship between general skeletal and oral bone findings. There was a correlation between skeletal osteopenia and residual ridge and alveolar bone density but no relationship between residual ridge reduction or periodontal disease and osteopenia was found. However, Lutwak et al. (1974) reported a correlation between severe periodontal disease and skeletal osteopenia in osteoporotic subjects with vertebral fractures. Kribbs et al. concluded that

the etiological factors in bone loss of the residual ridge and alveolar bone were multifactorial but that skeletal osteopenia does have oral effects.

Several studies have correlated osteopenic changes in the mandible with changes in other bones and have found that a relationship exists in some cases. Von Wowern and Melsen (1979) compared bone mass of mandible and iliac crest, and concluded that mass and cortical width in the mandible cannot be predicted from an iliac crest biopsy (or vice versa) perhaps due to different age-dependent functional changes of the two bones.

Henrikson and Wallenius (1974a&b) found a relationship between mineral density in the mandible and radius in both sexes, and also that changes with age qualitatively affected the mandible and radius in the same way with a decrease in bone mass.

A similar study was carried out by von Wowern (1985) in which bone mineral content (BMC) of the mandible was compared to that of the distal radius, using dual-photon absorptiometry (DPA). It was concluded that BMC of the mandible and distal radius must be corrected for sex and age and that BMC in the mandible and distal radius were significantly correlated. The mandible differs from other bones such as the lumbar spine and femur in that it has no weightbearing function and is formed through intramembranous ossification rather than endochondral ossification. For these reasons, the rate and magnitude of loss of mandibular BMC with sex, age, medical treatment, and diseases involving calcium metabolism, might be different from corresponding BMC changes in other parts of the skeleton (von Wowern et al., 1988). In studying the relationship between mandibular, forearm (radius) and lumbar spine BMC, von Wowern et al. (1988) found that there was a poor correlation between mandibular and lumbar spine BMC and between mandibular and radial BMC, using DPA. The reason given for the poor correlation between the mandible and other bones is that the mandible consists largely of cortical bone whereas the radius and femur contain more trabecular bone. Correlations between the mandible, forearm and femur were not investigated with plain radiography.

Using microradiograms, Von Wowern also studied variations in bone mass within cortices (1977a) and within trabecular bone of the mandible (1977b). Bone mass varied in the buccal cortex but was fairly uniform over the lingual cortex; the inferior cortex was not evaluated. There were marked variations in bone mass in trabecular bone within the same region in the mandible and variation in trabecular pattern between regions of similar bone mass. In the mandible, therefore, we can conclude that trabecular bone architecture is not a reliable indicator of generalized osteopenia and that in radiographic studies, the cortices must be evaluated. Either the premolar or molar regions of the mandibular body should be chosen as biopsy sites for comparative intramandibular analyses.

Weinstein & Hutson (1987) studied bone in the iliac crest and found, with advancing age (and presumably with development of generalized osteopenia), there was a decrease in trabecular bone volume, manifested as an increase in the distance between adjacent trabeculae and some decrease in trabecular thickness. Parfitt (1987) disputed these findings and argued that bone loss manifests as loss of trabecular connectivity and thickening of remaining trabeculae to compensate for the resulting loss of mechanical strength of bone. Pødenphant et al. (1987) studied vertebrae of osteoporotic patients and found trabecular bone loss and deteriorated trabecular microstructure. Unfortunately, these findings cannot be extrapolated to the mandible since its trabecular architecture is too variable, both intra- and inter subject, to serve as a reliable indicator of generalized skeletal osteopenia. However, the mandibular cortices show a more consistent pattern of change in generalized skeletal osteopenia.

Using plain films, the thickness of the mandibular angular cortex at the gonion in panoramic films has been suggested as an indicator of generalized bone loss (Bras et al. 1982a&b). Radiographs of both normal and osteopenic subjects in chronic renal failure were evaluated but no correction for film magnification or reproducible patient positioning was made in Bras' series, suggesting that the findings be interpreted with caution. In addition, no other cortices (eg. sinus cortex, inferior alveolar canal cortices) were evaluated

so effects of muscle pull on cortical thickness at the gonion were not considered. At the gonion, the masseter and medial pterygoid muscles attach to the lateral and medial aspects of the mandible respectively, potentially affecting cortical width measurements at this site. A similar study was carried out by Kribbs et al. (1990), where gonial cortical thickness was measured in fifty women and compared with SPA of the radius and DPA and QCT of the lumbar spine. It was found that cortical thickness at the gonion was significantly correlated with the other skeletal measures. However, Kribbs' study had the same limitations as Bras' series, thereby limiting the usefulness of the conclusions.

Mandibular ridge resorption and osteopenia

Osteopenia has also been linked to edentulous ridge resorption (Kribbs et al., 1983; Atwood and Coy, 1971; Mercier and Inoue, 1981; Habets et al., 1987; Bras et al., 1983, 1985; Ortman et al., 1989) but these studies did not focus on the radiographic appearance of osteoporotic changes per se. It is accepted that there is an association between skeletal demineralization and mandibular atrophy although the degree of correlation depends on the method used to evaluate mandibular bone loss and the method used to estimate skeletal osteopenia (Kribbs and Chesnut, 1984). Although the etiology of edentulous ridge resorption is unclear, alveolar bone seems to be highly sensitive to changes in systemic bone mineral content. Animal studies of osteopenia have shown that alveolar bone may be affected prior to the ribs, vertebrae and long bones, suggesting that alveolar bone loss may be an early indicator of generalized skeletal osteopenia (Bays, 1982). However, other studies do not support this finding; Mercier and Inoue (1981) found no relationship between bone density of the radius (as measured by SPA) and severity of edentulous ridge atrophy. Because the etiology of alveolar ridge resorption is multifactorial and difficult to account for in experimental studies, correlating ridge resorption and skeletal bone density may not be valid.

Age changes in the mandible

Several studies have documented age-related changes in the mandible (von Wowern and Stoltze 1978a, 1979a, 1980, 1982; Manson and Lucas, 1962; Atkinson and Woodhead, 1968) but no correlation with radiographic appearance in plain films was attempted. Von Wowern and Stoltze determined that cortical porosity and the percentage of Haversian canals showing resorption are unrelated to sex and increase after the age of 50. Mean cortical width and absolute bone mass are greater in males than in females and show a parallel age-related decrease after the age of 50. The authors concluded that age-related increase in cortical thinning and porosity is dependent on the individual as well as on age although there is marked individual variation. In addition, von Wowern & Stoltze found that coarseness of the bone trabeculae is independent of sex and age. Von Wowern concluded that because cortical porosity in the mandible increases with increasing age, cortical bone is useful for evaluation of age-dependent changes in bone mass in the mandible.

Atkinson and Woodhead (1968) also studied changes in the human mandibular structure with age and, like von Wowern, found that porosity of the mandible increases with age. Mandibular bone density was evaluated by using the technique of pyknometry (Archimede's principle) where the volume of a specimen of cortical bone is immersed in water and the resulting water displacement measured by a pyknometer. Atkinson and Woodhead found variations in porosity between the buccal and lingual cortices in different regions of the mandible. The more porous areas corresponded to those parts of the alveolus which are affected by age-related resorption, resulting in the characteristic altered dental arch shape seen in aged subjects. That is, bone density was decreased in the buccal cortex of the incisor region and in the lingual cortex of the molar region. The size of the porous region increases with age but the overall pattern is retained. In another study by Atkinson and Woodhead (1973), porosity and trabecular bone pattern in the vertebra, femur and mandible were examined. They concluded that the pattern of mandibular

porosity is present throughout life and is not a response solely to mechanical demand. Instead, the pattern is accentuated with aging and is thought to be a continuation of the modeling that originated during growth.

Mandibular measurement

Accurate radiographic measurement of the mandible requires measurement of a reproducible point in all specimens, and that this point is representative of the entire mandible. Von Wowern and Stoltze (1978b) established a standard technique for analyzing bone mass and bone activity in small, human jaw specimens and concluded that bone in the mandibular premolar-mental foramen area is suitable for histoquantitation and is representative of a larger area of the mandible. According to von Wowern and Stoltze, bone mass and bone remodeling, among other factors, are dependent on functional forces affecting a bone or part of a bone. In mandibular bone measurement, whether measurements are made from plain radiographs or from histologic slides, it is necessary to find an area which is stable from an anatomical and functional point of view. According to von Wowern, the area of the mental foramen best meets these criteria.

Vertebral measurement

In humans, vertebral "shape" or "geometry" has been studied. Hangartner et al. (1987) described a method for evaluation of lateral spine radiographs to quantitate changes in vertebral shape, and thereby screen for individuals at risk for osteoporosis. Davies et al. (1989) performed a similar study and found that shape and ranges of variability differ from vertebra to vertebra and that osteopenic bone is more difficult to measure because of the faint bony outlines visible in the radiographs. Despite these difficulties, quantitative measurement of vertebral shape is a useful adjunct in patient evaluation.

Animal models for osteopenia

Several animal models including the beagle, cat, and rat, have been used to study the physiological mechanisms leading to generalized skeletal osteopenia. The ideal animal model possesses a skeleton which has similar features to the human skeleton with respect to peak bone mass, remodeling at skeletal maturity, and low turnover and bone fragility in the senile skeleton (Jerome, 1987), however, a perfect animal model does not exist. At present, the two most widely-used animal models are the dog and the rat.

Dog

The dog, specifically the Beagle, is a good model for the study of adult human skeletal osteopenia. According to Martin et al. (1981), dogs are used for bone loss studies for the following reasons: (1) the dog skeleton is identical in composition and manner of bone remodeling to that of man; (2) the dog has well-documented normative values for numerous systems; (3) longitudinal studies are possible because of the large body size and long lifespan of dogs; (4) proven experimental models are available for studies in specific types of bone loss in dogs; (5) the time required for interventional studies is shorter than in man because of dogs' shorter lifespan and faster rate of bone turnover. Some disadvantages of the dog model of skeletal osteopenia exist, such as skeletal difference in relation to menopause, altered weight-bearing nature of a quadruped, cost, and availability. The female dog, unlike human females, does not undergo menopause, with the canine ovarian cortex remaining active throughout life (Snow, 1984). However, despite these differences, the dog model of skeletal osteopenia is probably one of the most useful.

Rat

The rat has remained the animal model of choice, due in part to its low maintenance cost and ease of handling. In addition, the adult rat skeleton possesses all the mechanisms needed to study induction of osteopenia except for microdamage production, (Jee, 1987)

however, several important differences between rat and human bone remodeling exist. The rat has a continuously growing skeleton in which the epiphyses never fuse. Unlike humans, remodeling of cortical bone is not thought to occur in the rat, so direct comparisons to human bone remodeling are not possible. However, Baron et al. (1984) feel that Haversian remodeling of cortical bone *does* occur but growth plates and primary spongiosa from measured areas must be excluded so that growth and remodeling remain separate. Baron et al. found that skeletal maturation in rats affects remodeling activity and this property can be useful when choosing experimental animals, particularly in examination of age-related changes in bone. Despite the fact that the female rat does not undergo classical bone remodeling and does not experience classical postmenopausal osteoporosis, it provides a model of skeletal osteopenia and is still useful in studies examining the pathophysiology of bone loss.

Problems of animal adaptation to dietary calcium deficiency have been encountered, making induction of skeletal osteopenia difficult in rats. In order to overcome this adaptive mechanism, pregnant, and/or lactating rats receiving calcium deficient diets have been used in order to induce an osteopenic state by sufficiently stressing the animals. Other methods of inducing skeletal osteopenia in rats have included ovariectomy with or without a calcium-deficient diet, administration of steroids, and limb splinting leading to disuse atrophy of the part.

Because of the widespread use and acceptance of the rat as a model of skeletal osteopenia, the following discussion will pertain only to rats.

Ovariectomy (OVX)

Osteopenia induced by ovariectomy (OVX) has been widely studied in the past. Hodgkinson et al. (1978) studied the effect of OVX and/or calcium deprivation on bone mass in rats and found that although OVX resulted in a reduction in bone mass, combining OVX with a calcium-deficient diet (CDD) resulted in the greatest effect on bone. Reduction

in cortical cross-sectional area and ratio of cortical to total area in the femur, reduced trabecular bone volume and increased percentage of osteoid surface in the tail vertebrae were noted. The effects of OVX on cortical bone were greater on a CDD than on a normal diet. Wronski et al. (1985, 1986) found that ovariectomized rats had reduced trabecular bone volume and accelerated bone turnover in the tibia and lumbar vertebra early after OVX. Bone loss was associated with elevated histomorphometric indices of bone resorption and formation. The data suggested that osteopenia in ovariectomized rats is more pronounced at skeletal sites with a greater relative increase in bone turnover, such as the tibia as opposed to the lumbar vertebra. The authors cautioned that the marked osteopenia noted in the proximal tibia may overestimate the magnitude of bone changes in the adult appendicular skeleton. For this reason, the lumbar vertebra was suggested as the superior sampling site for bone histomorphometric studies. Yamazaki and Yamaguchi (1989) found that the cortical thickness at the midshaft of the femur decreased progressively in rats ovariectomized at 52 weeks of age but no change in radiographic density of the midshaft resulted. Rats ovariectomized at an earlier age did not show these changes. On the other hand, Kimmel and Wronski (1990) found that osteopenia in ovariectomized rats is confined to a region containing appreciable cancellous bone and that the cortices remain relatively unaffected because rats do not exhibit cortical remodeling in the classic sense. Remodeling is the mechanism for bone replacement in the *adult* skeleton but because rats continue to grow indefinitely, they do not exhibit classical remodeling; instead, bone turnover is achieved through continuous modeling. Consequently, cortical remodeling in rats cannot be directly compared to that in other species and humans whose growth ceases. Baron et al. (1984) reported that skeletal processes in the vertebral column of growing rats are similar to the remodeling activity of adult bone and that the rate of bone turnover decreases in mature rats. The higher turnover rate in younger animals was attributed to a higher number or larger size of remodeling units and only partially to a higher formation rate at the individual cell level. In older animals, the reversal phase takes

longer with a slower turnover rate but the active resorption phase is slightly shorter, leaving the total duration of each remodeling cycle unchanged.

According to Kalu et al. (1984), the bone loss in ovariectomized animals is due to bone resorption exceeding formation. However, it is not clear whether OVX-induced osteopenia, and increased sensitivity of the skeleton of ovariectomized animals to the osteolytic action of parathyroid hormone (PTH), is due to a decrease in ovarian hormones, a decrease in calcitonin, a combination of both of these or to some other factors. Calcitonin is known to have a direct inhibitory action on osteoclastic bone resorption. Kalu also reports that ovarian hormone deficiency increases the sensitivity of bone to the osteolytic action of PTH, and the effects of calcitonin deficiency and ovarian hormone deficiency in sensitizing bone to the resorbing action of PTH appear to be additive. The model of pathogenesis of bone loss proposed by Kalu (1984) is as follows: Estrogen deficiency results in decreased renal synthesis of 1,25 $(OH)_2$ D_3 and thus, impaired vitamin D_3-mediated dietary calcium absorption, manifesting as hypocalcemia. The parathyroids are stimulated to secrete PTH in response to the hypocalcemic state although PTH is not itself required for increased bone resorption after the removal of the restraining influence of ovarian hormones. Decrease in serum calcitonin, secondary to ovarian hormone deficiency, will augment the already-increased skeletal sensitivity to PTH due to estrogen deficiency. Decreased serum calcitonin will also impair the conservation of dietary calcium after eating, further promoting a negative skeletal bone balance in estrogen deficiency.

Calcium-deficient diet (CDD)

The normal amount of dietary calcium recommended for rats is 0.5% (Larsson, 1969; Thomas et al., 1988). Studies examining the effects of a CDD vary widely in the amount of calcium actually included in the diet, ranging from 0% calcium to diets only moderately deficient in calcium. Stauffer et al. (1973) studied rats fed a diet with 0.01% calcium and found that osteoclastic bone resorption increased, probably due to the

induction of secondary hyperparathyroidism. There was also an increase in the rate of bone resorption on the endosteal surface as well as marked inhibition of matrix formation and mineralization. Harrison and Fraser (1960) reported similar findings; they also noted that a CDD (0.08% calcium) caused slower growth and weight gain in the experimental animals, and that upon dissection, the bones were brittle, opaque and white in color. Some of the rats sustained fractures and bone thinning was readily visible in the radiographs.

Thomas et al. (1988) studied the effects of 0.1% vs. 0.5% dietary calcium in rats, and found that animals fed a diet adequate in calcium (0.5%) maintained thicker bone cortices than those on the CDD and that the disparity between the groups increased with time. The degree of skeletal mineralization varied depending on the dietary calcium content. Thomas et al. suggested that in some experiments, animals should be maintained on diets containing lower calcium concentrations in order to prevent overwhelming the system with calcium, which might prevent the recruitment of regulatory processes which are only utilized under conditions of mild calcium stress.

Salomon (1972) found bone resorption in the metatarsals after seven days to nine months after the start of a CDD containing 0.02-0.03% calcium. The cortical bone decreased in thickness during the first month, increased slightly during the second month and then remained unchanged for the remainder of the experimental period. Salomon attributed the early decrease in thickness to subendosteal and subperiosteal resorption along with cessation of periosteal bone formation. The combination of resorption at both cortical surfaces accounts for the rapid thinning of the cortices and the decrease in the diameter of the shaft. As subperiosteal resorption ceases and new subperiosteal bone formation resumes and exceeds subendosteal resorption, the cortices thicken, explaining the increase in diameter seen in the second month. The new subperiosteal bone formation is transient and does not continue beyond the second month. Adaptation to the calcium deficiency occurs by the third month, accounting for the lack of change in the cortices seen after this period.

Increased total mandibular bone resorption is seen in rats fed a high protein, low calcium diet. The mandibles of these animals exhibit increased porosity and pitting at their surfaces. According to Sones et al. (1986), protein and calcium are both closely involved in bone metabolism. Diets deficient in protein result in "matrix osteoporosis" due to reduced deposition of bone reflecting a failure of osteogenesis at the stage of ossification. Conversely, diets deficient in calcium result in "mineral osteoporosis" where the deposition of bone matrix is normal but through the action of vitamin D and PTH, there is enhanced destruction of older bone so that calcium is released to supplement the inadequate dietary supply.

Pregnancy and lactation

The effects of pregnancy and lactation on rats receiving a normal diet were studied by Komarkova et al. (1967) and Warnock (1944). Komarkova found that serum calcium levels increased during lactation and decreased just before weaning and returned to normal 8 days after weaning. Phosphorus levels initially increased and then decreased during the period of lactation and then suddenly increased on the first day after weaning. Bone changes also occurred during lactation; resorption of spongy and compact bone was noted, despite administration of adequate amounts of dietary calcium. The calcium and phosphorus content of bones decreased during lactation along with decreases in bone dry weight and bone ash. The authors concluded that the rat skeleton is influenced by endogenous and exogenous factors during lactation and that lactation exerts greater demands on the animal than pregnancy. Warnock's (1944) findings agreed with those of Komarkova (1967) although Warnock concluded that the ends of the long bones were affected much more than the shafts. There was a significant reduction in the weight of the bone and the total quantity of ash at the bone ends throughout the period of lactation. It was also found that the bone shafts of lactating rats were not used as a mineral source to sustain the mammary supply during lactation, so it could be concluded that an osteopenic

skeleton is not an obligatory consequence of lactation if adequate dietary calcium is available. In addition, pregnancy per se did not deplete the stored minerals in bones; mineral stores were only depleted after parturition during the period of lactation, manifesting as resorption of the spongiosa. At the end of lactation, the rate of replenishment of spongiosa was the same, irrespective of whether the animals were pregnant again at that time.

Bawden et al. (1962, 1964) studied the effects of reduced dietary calcium during pregnancy in rats. They found that the calcium-deficient rats were able to make adjustments in their calcium metabolism in order to supply the fetuses with calcium in amounts similar to the control animals. The was achieved by:

1. Increased retention of dietary calcium.
2. Increased net resorption of bone to maintain blood calcium levels. Bone which existed before pregnancy was a major source of calcium withdrawal in the maternal skeleton.

Rasmussen (1977a&b) studied the effects of pregnancy and lactation on the skeleton of calcium-deficient rats; he concluded that lactation (not pregnancy alone) represented the heaviest physiological load on the calcium homeostatic mechanism. Rasmussen also found that bone mineral and percentage ash of the long bones were reduced in pregnant rats fed a calcium-deficient diet. The bone loss was accentuated in the ends of the femurs rather than affecting the entire bone equally and these changes were more prominent in lactating rats. The changes observed in the long bones of such rats included almost complete loss of bone trabeculae from the metaphysis, partial loss and thinning of the trabeculae of the epiphysis and reduced thickness of the diaphyseal cortex.

In a similar study (Hagaman, 1990), it was found that at the end of lactation, regardless if the rats were fed a CDD or normal diet, there was a large loss of trabecular bone, increased porosity of endosteal surfaces and cortical thinning of the midshafts of the femora. These changes were more marked in the CDD rats. If adequate levels of calcium

were administered immediately after or three weeks after lactation, the bone recovered, manifesting as increased bone mineral, increased thickening of the diaphyseal cortex and smoothing of the endosteal surface.

Ellinger et al. (1952) found that there were cycles of erosion of bone during lactation and repair (formation of new bone) after the period of lactation, and during the subsequent gestation, even in rats receiving adequate dietary calcium. Administration of a CDD has no effect on longitudinal bone growth unless the diet was severely deficient in calcium (0.04%). The CDD only had a moderate effect on lactation. It was found that different parts of bones contributed different quantities of mineral during the resorption phase:

1. Zones rich in cancellous bone (eg. head and metaphysis of femur, head of tibia) are the prime sources of mineral and therefore are most likely to resorb. The vertebrae were not studied but because the vertebrae have a high content of cancellous bone, they would likely also show marked resorption of their internal surfaces.
2. Zones principally composed of compact bone (eg. shaft of femur, shaft and distal portion of tibia) are less subject to resorption unless the diet is extremely low in calcium.

El-Maraghi et al. (1965) also found that a CDD did not affect the growth of the femurs or other bones although these bones had a lower radiographic density than those of control animals.

Miller et al. (1989) examined cancellous bone remodeling during lactation in beagles and found that during this time, like in rodents, bone remodeling and bone turnover are increased. The reason for this may be due to the "reversible mineral deficit" (RMD) described by Parfitt (1980) which may be the physiological mechanism to augment calcium stores with minimal impact on skeletal structural integrity. An increase in bone remodeling

will remove the older, more highly mineralized bone and replace it with new bone that will progressively mineralize. The increase in bone remodeling yields a transient net loss of skeletal calcium and provides a greater volume of partially mineralized bone, thus increasing the exchangeable calcium pool in the skeleton.

Although lactation is known to affect BMC in calcium-deficient rats, the number of suckling pups is an important influence on the degree and pattern of BMC loss because with a larger number of pups, the calcium drain will be greater (Peng et al., 1988). Rats suckling a large number of pups (7-11 pups) exhibited bone loss evenly distributed along the whole length of the femur. Rats suckling fewer pups (2-3 pups) exhibited more bone loss in the metaphyses than in the midshaft. If the lactating rats were fed a CDD, the mechanical properties of the femurs were adversely affected.

Human studies, unlike the rat studies described above, indicate that lactation history is not associated with significant differences in bone density in the wrist, spine or hip, despite variations in calcium intake (although the subjects all consumed adequate amounts of calcium), weight or duration of lactation (Koetting and Wardlaw, 1988). Only height was correlated to bone density of L2-L3.

Age-associated osteopenia in rats

As in humans, the rat skeleton undergoes specific, age-related changes manifesting as osteopenia. Kiebzak et al. (1988) studied these age changes and concluded that bone mineral loss with age is site-specific in the rat femur, with the metaphysis (consisting mostly of cortical bone) losing more BMC than the distal diaphysis (consisting mostly of trabecular bone) in old rats. The width of the femur increased and the bone density decreased with increasing age.

Aging female rats are known to lose significant amounts of trabecular bone volume (TBV) in the lumbar vertebrae and this loss is correlated with a decrease in BMC. Safadi et al. (1988) found that the TBV of old rats was 36.3% lower than that of normal young

adults and the BMC of old female rats was 25% lower than that of young adults of the same sex.

Bar-Shira-Maymon (1989) discussed age-related osteopenia and suggested that it involves not only skeletal tissues but systemic and/or local regulation of minerals as well. Increased rates of osteoclastic activity and abnormalities of bone formation are involved in progressive loss of bone mass. According to Bar-Shira-Maymon, these phenomena may be due to an age-related decrease in the number of bone cells as well as to a decrease in osteoblast renewal or a loss of the template for formation. In addition, aged rats absorb less calcium than younger animals and the renal mitochondria from aged rats synthesize less 1,25 $(OH)_2$ D_3 than younger animals.

Experimental problem

The evidence to date suggests that changes in mandibular bone mass may reflect generalized skeletal changes, however, previous reports published in the dental literature consist of clinical ad hoc cross-sectional studies in which methods other than plain film radiography were used to assess mandibular bone mass. A carefully-controlled scientific study of the mandibular cortices is necessary in order to determine if mandibular cortical width measurements can indeed be used as a guide to determine if skeletal osteopenia is present. If a radiographic correlation between mandibular cortical thickness and cortical thickness of the femur or vertebrae is found, this information could be useful in screening patients for osteopenia in the dental office. By observing changes in the mandibular cortices with progression of osteopenia, this information could have useful clinical value in predicting which edentulous patients might undergo excessive ridge resorption. In order to determine if such correlations exist, an animal model of osteopenia must first be defined

and the extent of correlation between the various bones, if any, determined and the changes over time documented.

The present study was undertaken to determine if radiographic changes, specifically cortical thickness, in the mandible, femur and first lumbar vertebra of osteopenic female rats were correlated with each other and with the duration of the osteopenic state. Osteopenia was induced in the experimental groups by administering a calcium-deficient diet to lactating rats. Animals were divided into five experimental groups and sacrificed over a period of nine months. A control group of virgin rats on a normal diet served as a baseline for the study. Each experimental group was further subdivided into three treatment groups; the first consisting of virgin rats on a normal diet (control group); the second consisting of bred rats on a normal diet; and the third treatment group consisting of bred rats on a calcium-deficient diet, for a total of thirteen subgroups. The mandible, both femurs and the first lumbar vertebra for each rat were radiographed in two positions and various parameters measured in these plain films using a computer digitizing and analysis system. The data were then statistically analyzed to determine if the radiographic appearance of specific sites in the mandible correlated with those of the other skeletal sites in the presence of skeletal osteopenia.

It is hypothesized that all of the measured cortical widths in osteopenic animals will decrease, more so in animals which are osteopenic for a greater length of time. In addition, mandibular cortices should decrease in width to the same extent as those in the femur. Cortical widths for bred rats on a normal diet should correspond with cortical widths for virgin rats on a normal diet since after weaning, no other physiological stress to calcium metabolism is present in the bred rats on a normal diet.

Although the rat is a quadruped, the geometry of the first lumbar vertebra will be studied to determine if there is any change in vertebral shape with the onset of skeletal osteopenia.

Chapter 2

Experimental Design and Methodology

One hundred and fifty-five female, ninety day-old Sprague Dawley rats* (mean weight = 258g ± 17g) were studied over a period of nine months. The initial age was selected because it represents early adulthood, thereby removing potential bias due to active growth or old age. All rats were virgins; 95 of these were bred for the first time for this study. The rats were housed in standard cages, three animals per cage. Bred rats were housed singly until their pups were weaned, and then in groups of three per cage. In a randomized, complete block design, rats were allocated to three treatment groups (n = 12), at each of 5 study periods over 9 months. At each of these 5 time points except the first (at which only 12 rats were sacrificed), 36 rats were sacrificed (Table 2.1)

Table 2.1 Experimental design and sacrifice schedule.

	Age at sacrifice				
	12 wks (baseline)	18 wks	24 wks	36 wks	48 wks
Treatment group VND	n = 12	n = 12	n = 12	n = 12	n = 12
BND	*	n = 12	n = 12	n = 12	n = 12
BLC	*	n = 12	n = 12	n = 12	n = 11

VND = virgin, normal diet; BND = bred, normal diet; BLC = bred, low calcium diet
* = only 12 animals (VND) in the group sacrificed at 12 weeks

* Biological Sciences Animal Services, University of Alberta

The baseline sacrifice group (n=12), were all 12 week-old VND rats, and these served as the baseline control for all three treatment groups.

Each treatment group at each time point after baseline consisted of 12 rats, except for BLC animals sacrificed at 48 weeks, which had only 11 animals because one of the rats was later found not to be pregnant and was not included in the study.

Rats in the VND and BND treatment groups were fed a normal diet containing adequate (1.46%) calcium (Appendix A) for the duration of the study until sacrifice. Rats in the BLC treatment group were fed the normal diet until the day of parturition and were then changed to a calcium-deficient diet (CDD) consisting of 0.1% calcium (Appendix A) for the duration of the study until sacrifice. All rats received food and tap water ad lib. Shortly after parturition, the litters in the BND and BLC treatment groups were adjusted to 12 pups per mother and then weaned after 3 weeks.

All rats were weighed weekly from the first day of the study, except the bred rats were weighed weekly beginning immediately after weaning due to difficulty in handling during the period of nursing.

Before sacrifice, 5 rats from each treatment group, (total of 65 rats) were selected for dynamic histomorphometry studies. VND rats were chosen randomly; BND and BLC animals were randomly selected from those rats which still had 12 pups at the end of the weaning period in order to ensure that the calcium demand was equal.

Rats selected for histomorphometry received two subcutaneous injections of tetracycline to label bone for fluoroscopic microscopy with the following schedule:

1. Tetracycline HCl (hydrochloride) 10 days before sacrifice, 25 mg/kg of body weight.
2. Calcein (Sigma Chemical Co., St. Louis, MO) 2 days before sacrifice, 10 mg/kg of body weight.

The histomorphometry data are beyond the scope of this thesis and will be reported separately.

Rats were sacrificed by CO_2 asphyxiation; the mandible, both femurs and first lumbar vertebra were removed by blunt dissection and soft tissue by mechanical scraping. The right femur and right mandible were immediately placed in 70% ethanol for subsequent plastic embedding (Spur's Low Viscosity Embedding Kit, Micro Biological Supplies, Richmond Hill, Ontario); the remaining bones were stored frozen in plastic freezer bags to prevent dehydration.

Radiographic Examination

The mandible, femurs and first lumbar vertebrae were each radiographed twice in the geometries described below, using an extraoral C-arm x-ray unit (Elema-Schönander, Stockholm-Solna, Sweden) with a 0.3 mm diameter focal spot. High detail single-emulsion mammography film (Kodak NMBI 1 film) with a Kodak fine Lanex regular screen were used for all views. One set of radiographs was taken with the specimens in contact with the film cassette and a tube-object distance of 53.2 cm. These data are reported as the "standard" (unmagnified) views. The second set of radiographs were taken by placing the bones on an acrylic platform positioned on the cassette. The tube-object distance was 43.2 cm, the object-film distance 10 cm. (Fig. 2.1) These data are reported as the "magnified" views.

The alignment of the x-ray tube with the cassette and with the acrylic platform was verified by making a test exposure using an acrylic phantom which was 25 mm in diameter and 15 cm high; the rod was attached to an 8.5 mm thick base and a 1.5 mm wide, 0.5 mm thick metal ring was recessed into each end of the rod, flush with the outer surface of the rod (Fig. 2.2). Separate exposures of the phantom were made with the phantom resting on the cassette (as in the standard views) and with the phantom placed on the acrylic platform

(as in the magnified views). Because of the height discrepancy between the two metal rings, the upper ring was magnified; when the tube-film or tube-platform-film alignment was correct, the image of the lower ring was centered within the image of the upper ring.

For all mandibular and femoral views, except the mandibular occlusal views, the right and left sides were radiographed in separate exposures on different parts of the film. In mandibular occlusal views, the right and left sides were radiographed together as a single exposure. Soft wax (Modern Materials® Wax Square Ropes #94491, Columbus Dental, St. Louis, MO) was used as necessary to support the specimens. An 8 x 10 inch film cassette was divided into quarters and four exposures, one in each quarter, were made on each sheet of film. Parts of the film not used for a particular exposure were covered with lead blockers.

The specimens were positioned as follows for both standard and magnified views:

1. Mandible
   a) Left and right lateral views using 40 kVp, 50 mA, 2/5 sec

      The hemi-mandible was positioned flat on the cassette (or on the acrylic platform for the magnified views) with the buccal (cheek) surface of the mandible facing the x-ray tube.

   b) Left and right occlusal views using 40 kVp, 50 mA, 2/5 sec

      The two hemi-mandibles were supported with wax so that they were in an upright position with the inferior border of the mandible resting on the cassette (or acrylic stand). The occlusal plane of the posterior teeth was used as a guide for lateral-medial positioning of the mandibles so that the occlusal plane was parallel to the film cassette.

2. Femurs

   a) Left and right lateral views using 40 kVp, 50 mA, 1/2 sec

      Each femur was positioned flat on the cassette or acrylic platform with its lateral surface facing the cassette and the head of the femur on the tube side. The femur was rotated until, when viewed end-on, the intercondylar area was parallel to the cassette with the lateral and medial condyles aligned vertically.

   b) Anterior-posterior (A-P) views using 40 kVp, 50 mA, 1/2 sec

      The femur was positioned flat on its posterior surface and the posterior surfaces of both condyles in contact with the cassette or acrylic platform.

3. First lumbar vertebra

   a) Lateral view using 40 kVp, 50 mA, 1/2 sec

      The vertebra was positioned on its lateral side and rotated until the plane of the spinous process was parallel to the cassette.

   b) Posterior-anterior (P-A) view using 40 kVp, 50 mA, 1/2 sec

      The vertebra was positioned on its ventral aspect with the spinous process facing the x-ray tube. The specimen was rotated until the spinous process was perpendicular to the cassette.

   c) Transaxial view using 40 kVp, 50 mA, 1/2 sec

      The vertebra was positioned on its caudal aspect . The spinous process was used as a guide for proper tilt and aligned perpendicularly to the cassette.

The bone specimens for each animal were always oriented in the same way and exposed on the same parts of the film in order to eliminate the possibility of variation in data due to screen variation or heel effect from the anode. Each specimen was exposed

with an aluminum stepwedge and a brass/aluminum plate (Ritchie 1979), oriented in the same way for all of the exposures (Fig. 2.3). The aluminum stepwedge was used as a standard to allow for densitometric comparisons at a later date; the brass/aluminum plate was used to ensure that film quality, exposure and developing were constant.

The aluminum stepwedge was 60 mm long and 10 mm wide with a step width of 5 mm. In order to extend the gray scale of the wedge, a 0.5 mm thick 5 mm wide piece of aluminum was affixed to the back of the wedge on one side.

The brass/aluminum plate was 25 by 25 mm square. A total of nine - 1 mm diameter holes were placed with the centers 2 mm apart on a 0.5 mm thick brass grid which was covered with 4 mm of aluminum (Fig. 2.4).

All of the films were developed under well-standardized conditions using a Kodak RP X-OMAT develop

Radiographic Measurement

Preliminary film marking

Before the radiographic images were measured, preliminary film marking was done, as described below.

1. Lateral mandibular views

   Using a fine lead pencil, a straight line was drawn superimposed over the long axis of the pulp chamber of the distal root of the first molar, intersecting the inferior cortex of the mandible. This line was drawn on all the lateral mandibular views to ensure that cortical measurements were taken in the same relative area for all of the mandibles. If the line was not exactly superimposed over the pulp chamber, measurement error could

result. A second line was drawn at the alveolar ridge crest between the first and second molars in order to aid visualization of this thin cortex in the digitized images.

2. Lateral and A-P femoral views

Femoral cortical measurements were made at the midpoint of the long axis. To find this midpoint, a line was drawn in the center of the femur, along its long axis. Lines were then drawn perpendicular to the axis line at the extreme proximal and distal ends. These perpendicular lines were used to measure the femoral length with Vernier calipers (Digi-matic 6" calipers Series 500-321, Mitutoyo Corp., Japan). Five length measurements per specimen were obtained, averaged and halved to yield the midpoint measurement and then a line was drawn perpendicular to the long axis at the midpoint.

3. Vertebral views

Pencil lines were drawn parallel to the cortical edges of the caudal and rostral aspects of the vertebral bodies in order to aid visualization of the edges of these thin cortices in the digitized images.

Image digitization

The radiographic images were backlit using a standard viewbox in a darkened room and digitized using a black and white video camera (Hitachi VK-350) equipped with a macro lens (Macro-Switar f1.1 26 mm, Bolex, Switzerland) connected via a frame-grabber to a Macintosh IIcx computer. The software used to analyze the images was IMAGE Version 1.22 (Wayne Rasband, National Institutes of Health).

Radiographs were oriented so that the region of interest (ROI) was centered on the computer screen, corresponding to the area of greatest resolution. Once an image was digitized, it was frame-averaged (16 frames) in order to reduce noise. Brightness and

contrast were adjusted to obtain optimum viewing quality, and then image analysis was carried out.

Image analysis

Before analysis of the radiographic images, the imaging system was calibrated using a metal/acrylic line-pair grid, in order to accommodate for image magnification by the video camera. On average, there were 51± 2 pixels/mm, although this figure changed depending on camera distance from the film and therefore, the degree of magnification.

Once the system was calibrated, the radiographic images were digitized and analyzed. The cortical measurements were recorded by the computer program and then transferred directly into a spreadsheet (Microsoft Excel, Version 2.0).

Parameters measured in the images

For the mandibular, femoral and vertebral views, the following parameters were measured five consecutive times for both the standard and lateral views:

1. Mandible
   a) Lateral mandible (Fig. 2.5)
      i. height of the alveolar bone, measured from the crest of the alveolar ridge to the superior cortex of the inferior alveolar canal midway between the first and second molar teeth.
      ii. width of the inferior cortex of the mandible, measured along the line drawn along the long axis of the pulp chamber of the distal root of the first molar tooth.

b) Occlusal mandible (Fig. 2.6)

All of the occlusal mandible measurements were taken at a point directly anterior to the first molar tooth.

i. width of the buccal cortex

ii. width of the lingual cortex

iii. total width of the mandible

2. Femur

All of the femoral measurements were taken at the midpoint of the femur.

a) Lateral femur (Fig. 2.7)

i. width of the anterior cortex

ii. width of the posterior cortex

iii. total width of the femur

b) Anterior-posterior femur (Fig. 2.8)

i. width of the lateral cortex

ii. width of the medial cortex

iii. total width of the femur

3. Vertebra

a) Lateral vertebra (Fig. 2.9)

i. anterior-posterior width of the vertebral body, measured on the rostral aspect

ii. length of the vertebral body (described as anterior height of the vertebral body), measured on the ventral aspect

b) Posterior-anterior vertebra (Fig. 2.10)

i. length of the vertebral body, measured parallel to the spinous process (described as midbody height)

Precision of the measurement technique

To determine the precision of the measuring technique, a single set of femoral, mandibular and vertebral images were digitized and measured at 10 occasions throughout the image analysis process. Analysis of variance was used to determine the degree of variability in the repeated measures of these variables.

Accuracy of the Measurement Technique

To determine the accuracy of the measurement technique and to ensure that film quality, exposure and developing were constant, radiographic images of a brass plate were measured and compared with direct measurements of the brass plate. Twenty radiographic images of the brass plate were selected at random from all of the radiographic views in the study and digitized with the CDS. For each of the twenty images, the width of each hole (circle) and interval between the circles was measured five times each on both horizontal and vertical axes. The measurement direction alternated from left to right on the horizontal axis and from top to bottom on the vertical axis. This procedure was repeated for the actual brass plate, which was digitized and measured in the same manner as the radiographic images using the CDS.

The data was analyzed using repeated measures analysis of variance.

Reproducibility Study

Reproducibility in repositioning the same bone on the cassette for the standard views, and on the acrylic platform for the magnified views, was determined by the following experiment.

The left femur, mandible, and first lumbar vertebra from one rat were used in separate radiographic exposures in the same orientations as previously described. For the lateral mandibular views, only the right half of the mandible was radiographed. The same film/screen combination, exposure factors, and tube/object/film distances used for the experimental animals were used for this part of the study. Both standard and magnified views were taken of the specimens using the acrylic platform for the magnified views. For each set of standard views, a clear unexposed sheet of 8" x 10" film was affixed to the surface of the film cassette and marked into 17 squares. The bone specimen was then positioned in the center of the first square and supported with soft wax. The remainder of the cassette surface was covered with lead blockers before the exposure was made. The bone was then removed and repositioned in the next square, and as before, the lead blockers were placed and the exposure made. This procedure was repeated until all 17 exposures were completed. Magnified views were made in the same manner except that the specimens were placed on the acrylic platform in order to increase the object/film distance.

Radiographic analysis

The same variables as measured in the experimental groups were analyzed. Three methods (two manual methods and the computer-based method) of radiographic measurement were completed and compared. The first method was manual measurement of the mandibular and femoral views using a film viewbox and an optical grid (10X magnification Nikon eyepiece with F 2.8/50 Carl Zeiss lens). The second method was a manual measurement of the vertebral views using Vernier calipers. All measurements were

then repeated using the computer-based image analysis system. Each variable, for each of the 17 images on the sheet of film, was measured five times.

Statistical Design and Analysis

Determination of sample size

In order to ensure that measured changes in cortical widths of the experimental animals were not due to chance, an appropriate sample size had to be chosen. In choosing the sample size, it was assumed that the average expected change in cortical width would be 2%; a value based on the published results from other investigators.

Sample size was calculated using the following formula: (Sokal & Rohlf)

$$N = \frac{\sigma^2_D [Z_\alpha + Z_\beta]^2}{\delta^2}$$

Where, in a one-tailed test:

N = required sample size

σ_D = standard error of the population estimated from previous experiments

$\alpha = 0.05$

$\beta = 0.2$ (power $P' = 1-\beta = 0.8$)

Z score

δ = effect size (difference expected in the study, based on empirical investigations) = 2%

For the sample size calculation, we assume, for the rat, a homogenous bone response to pregnancy, lactation and inadequate levels of dietary calcium. We use a function of the sample standard deviation (s) as the standard error (σ_D) of the study population.

A conservative estimate of effect size (δ) is 2% , then σ_D is $\sqrt{2}$ x 1.5%:

$$N = \frac{6.2 \times 2(1.5)^2}{2^2} = 6.97 = 7 \text{ animals}$$

Depending upon the homogeneity of the sample response over time, 10 animals per subgroup would provide appropriate power; to compensate for drop-outs and other contingencies (eg. possible lack of homogeneity in sample variance, or differences from estimated changes over time), a sample size of 12 animals per treatment group was used.

Statistical analysis

Reproducibility study

The reproducibility study was analyzed using analysis of variance (ANOVA) and subsequently, the average coefficient of variation (percent standard deviation, CV%) was calculated for each variable. Paired t-tests were used to compare data from the different analysis methods.

Animal weights

ANOVA was used to determine the variability between matched treatment groups and between different treatment groups at various times during the study.

Litter size

ANOVA was used to determine the variability in the number of live pups left at weaning for all of the bred rats.

Bone analysis

Comparison of cortical width measurements for each bone over time within and across treatment groups was done using ANOVA. The Tukey HSD (honestly significant difference) test was used to determine which treatment groups differed, in cases where the null hypothesis was rejected. In cases where variance was not homogenous, appropriate non-parametric tests (eg. Kruskal-Wallis) were used to compare group mean values. Analysis of covariance was carried out to examine the influence of weight and age on the cortical width measurements; regression was also adjusted for covariance. Bonferroni probabilities were used to determine the degree of correlation between standard and magnified views.

The statistical tests compared each treatment group with the other treatment groups, thereby observing a progression of changes over time with each subsequent treatment group. Baseline animals (VND animals aged 12 weeks) and animals sacrificed at later dates were treated as if one animal was observed throughout the course of the experiment. That is, it was assumed that the entire population of rats in each particular treatment group were homogenous and that the changes seen would be uniform throughout the population.

Fig. 2.1. Acrylic stand used for the magnified views.

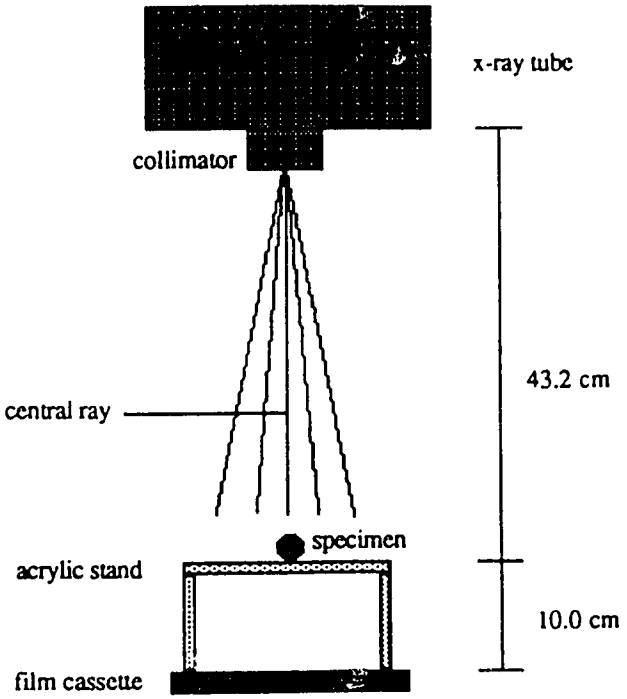

Fig. 2.2. Acrylic phantom used to check machine alignment.

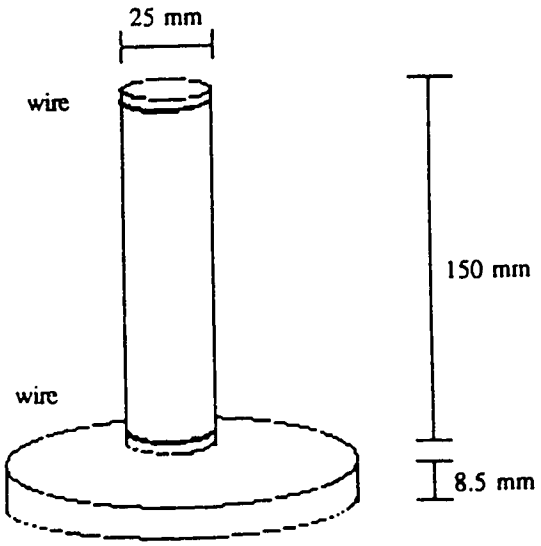

Fig. 2.3. Aluminum stepwedge exposed with each specimen.

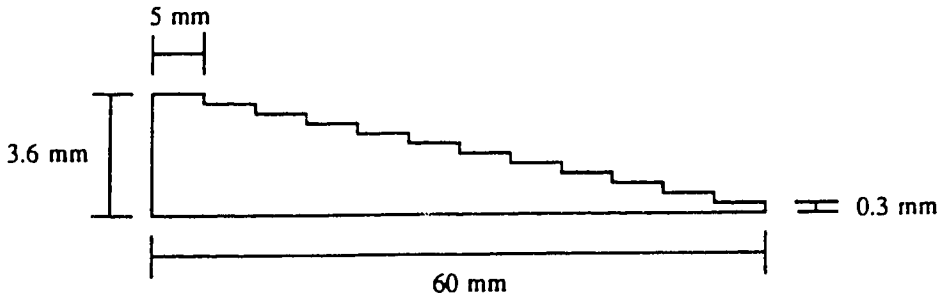

View of the aluminum stepwedge from the side (not to scale)

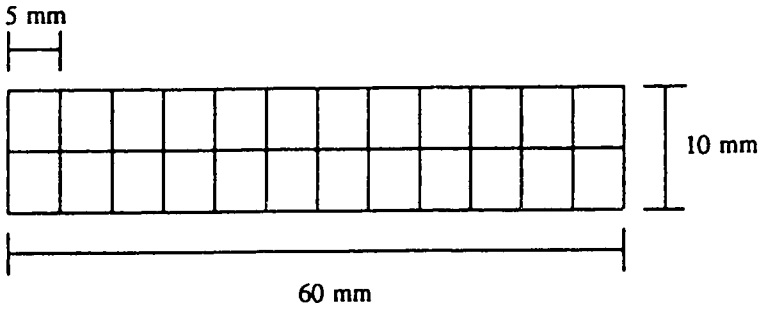

View of the aluminum stepwedge from the top (not to scale)

Fig. 2.4. Brass plate for quality control of x-ray exposure and film developing process.

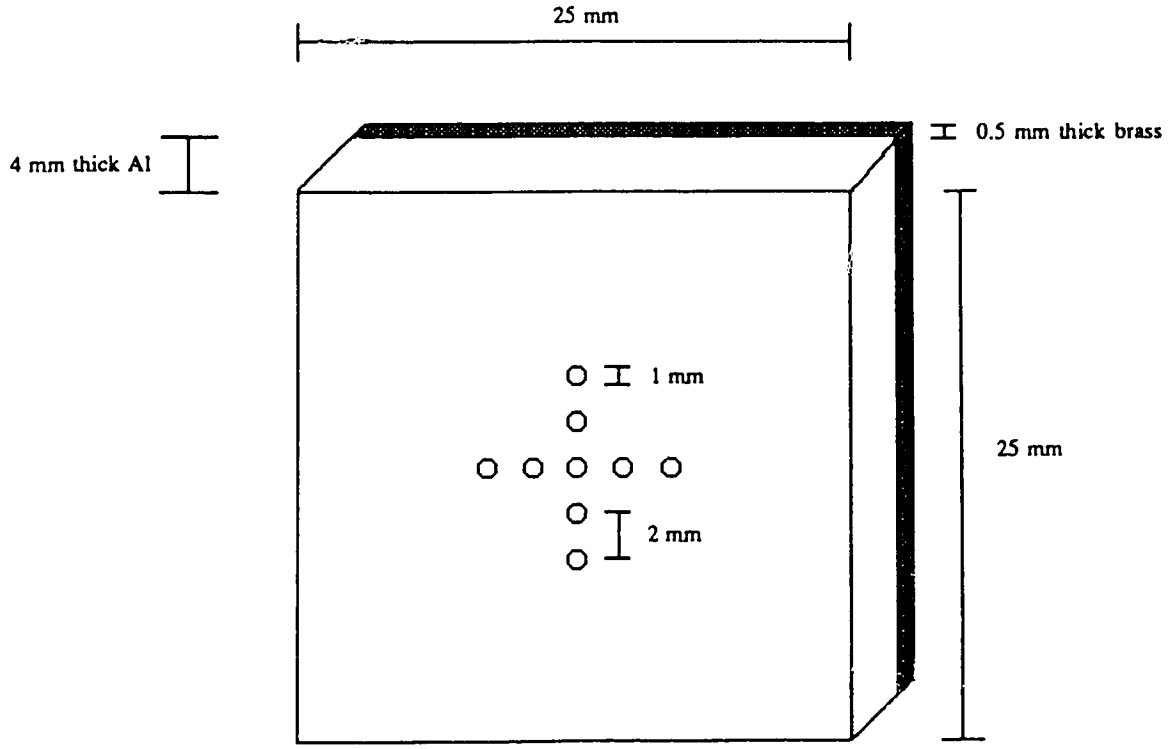

Fig. 2.5. Lateral mandible illustrating pencil lines used as guides for locating measurement sites.

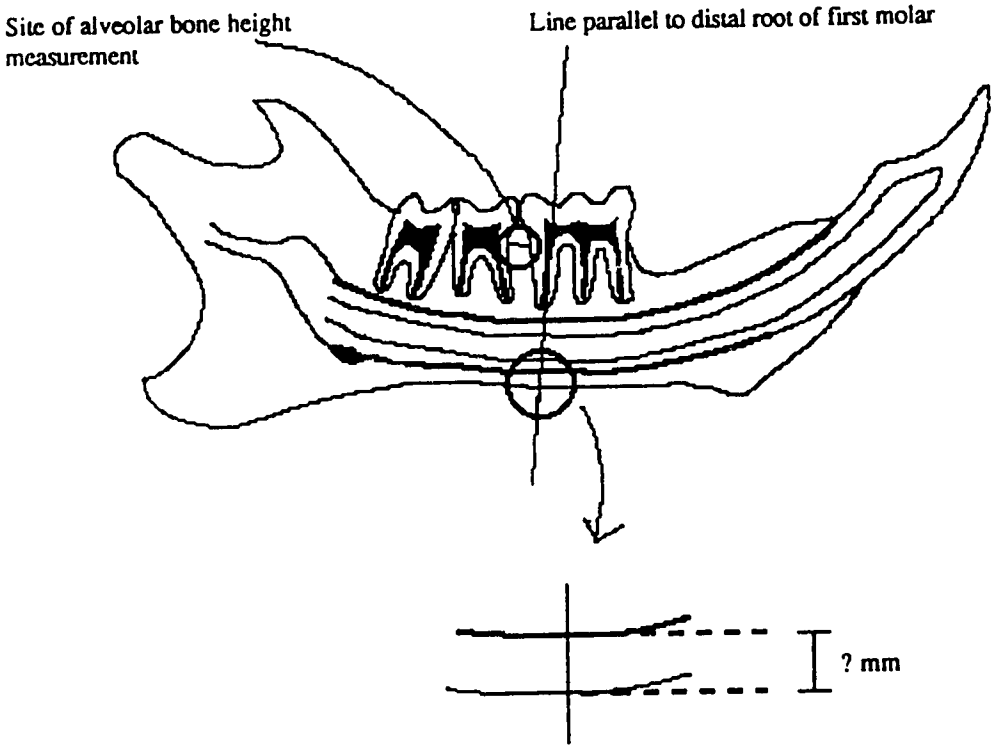

Fig. 2.6. Occlusal mandible illustrating the pencil line used as a guide for locating measurement sites.

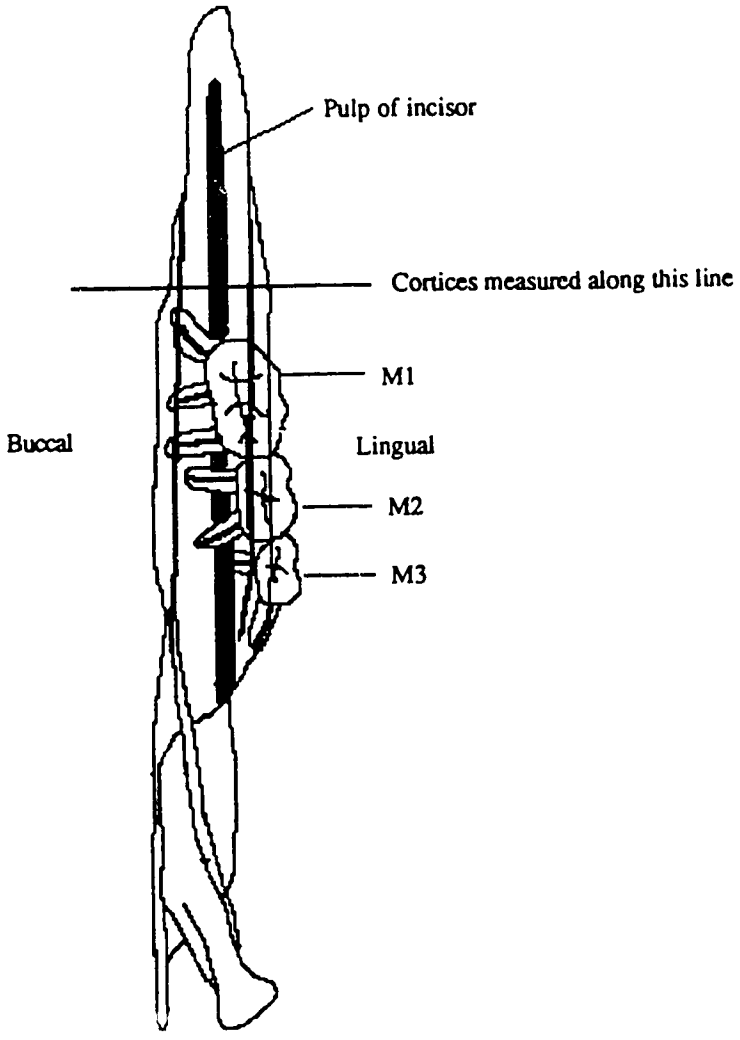

Fig. 2.7. Lateral femur illustrating method of locating the midpoint.

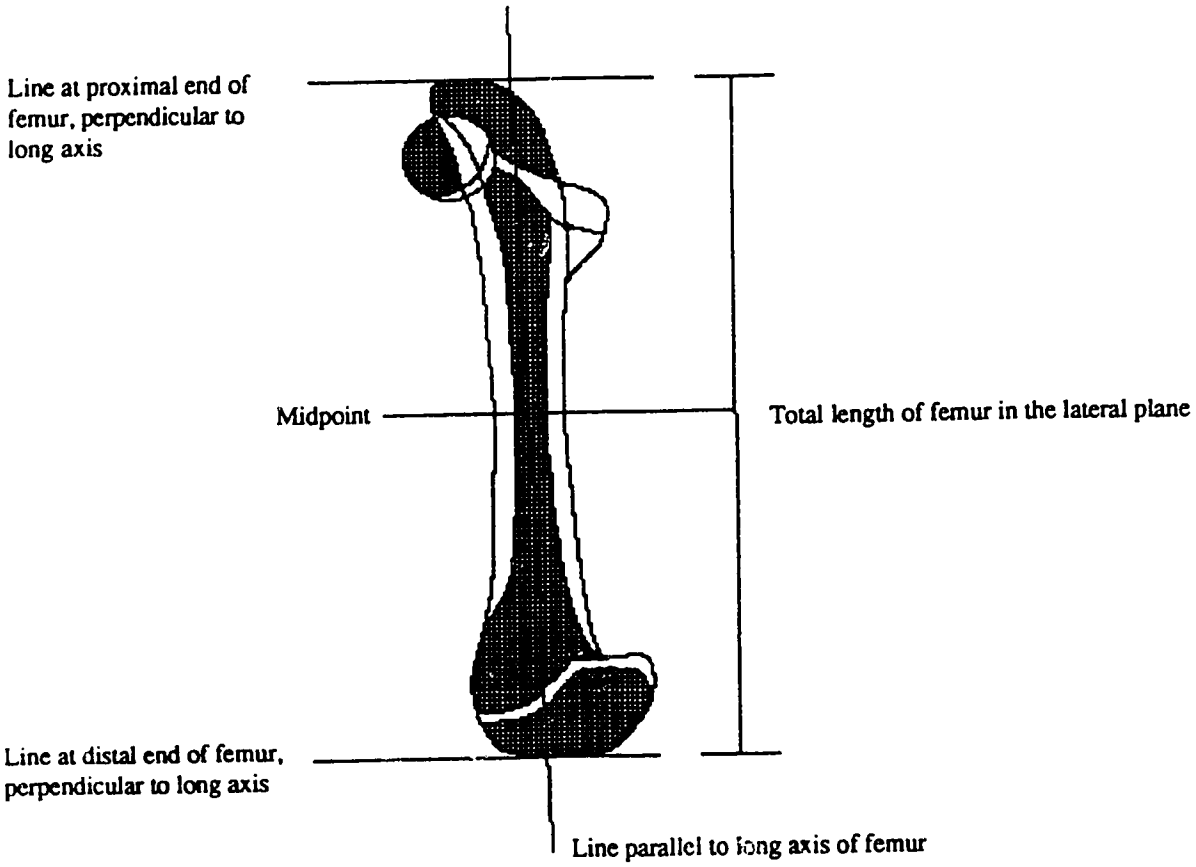

Fig. 2.8. Anterior-posterior femur illustrating method of locating the midpoint.

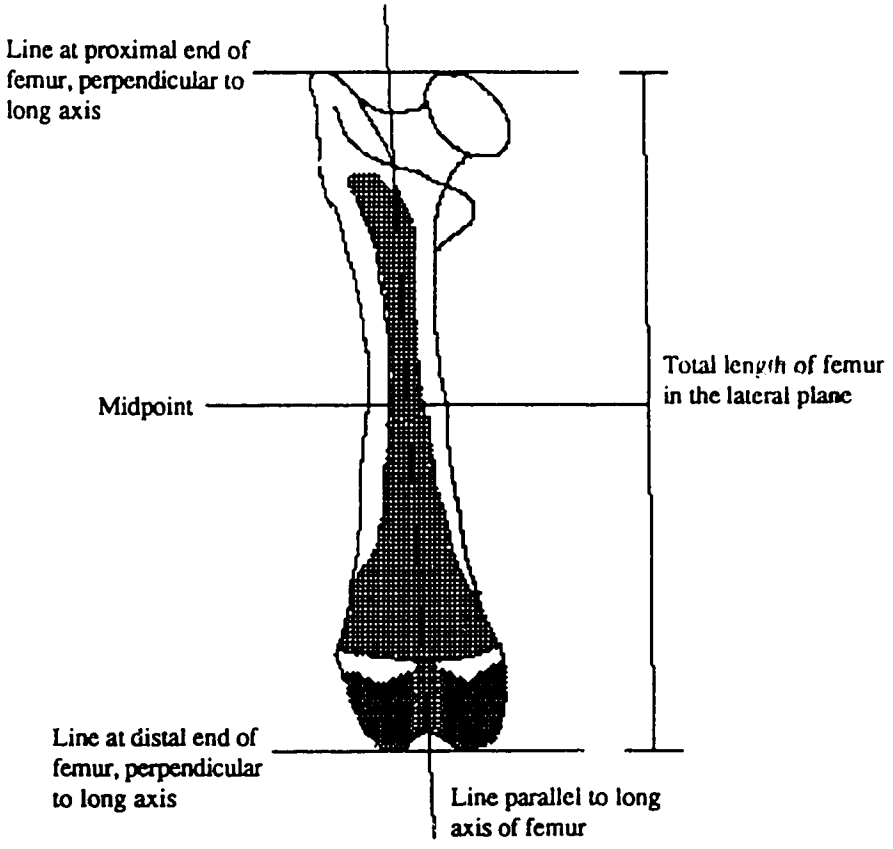

Fig. 2.9. Lateral vertebra illustrating method for measuring the anterior height.

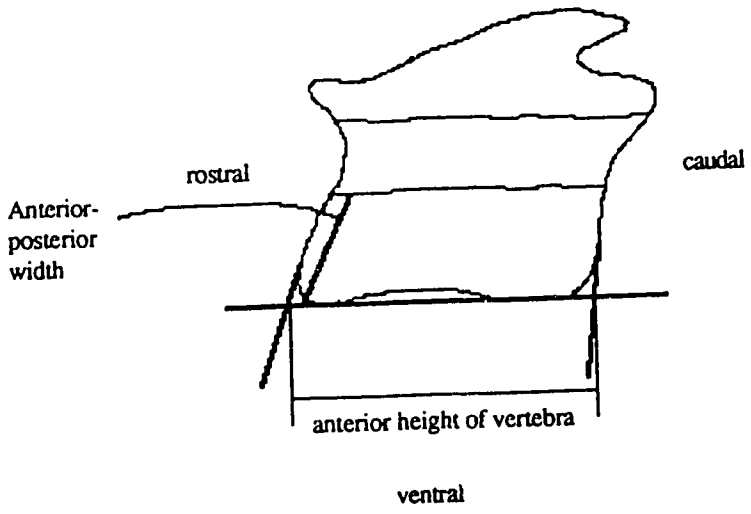

Fig. 2.10. Posterior-anterior vertebra

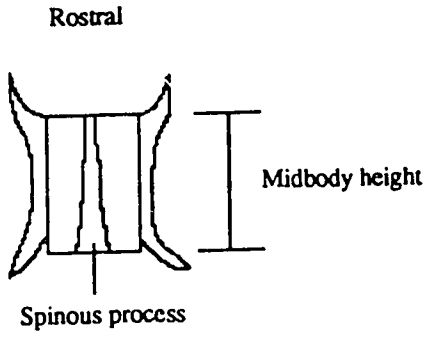

Chapter 3

Results

Reproducibility Study

The reproducibility of repeated specimen positioning and cortical measurement was tested in order to determine the degree of variation which might be expected from technique factors (positioning and measurement) alone.

Calipers

Standard and magnified anterior and midbody heights of vertebrae were quickly and easily measured using calipers. Analysis of variance (ANOVA) for each variable indicated that there were no significant differences between measurements except for magnified anterior vertebral height ($p = 0.03$). Coefficients of variation were calculated and are shown in Table 3.1.

Optical grid system (OGS)

The optical grid system (OGS) for cortical width measurement was simple to use, although operator fatigue made data collection difficult when a large number of films was measured at one session. Repeated measurements of cortical width for all bones were compared using ANOVA which indicated that specimen positioning, radiographic and measurement techniques were consistent; there were no significant differences in data when all the measurements for a particular variable were compared.

Computer digitizing system (CDS)

At the beginning of the study period, only calipers and the OGS were available for image measurement but later, the computer-based digitizing and measuring system (CDS) became available, so it was included in the reproducibility study. Although the OGS had lower coefficients of variation for some variables, it was decided to use only the CDS for image measurement of the experimental animals.

The CDS was also simple to use and had the advantage of allowing direct transfer of data into a computer spreadsheet, thereby eliminating the need for manual data entry. Cortical boundaries were visualized in greater detail with the CDS than with the optical grid system due to enlargement of the images. However, the more prominent edge gradients with the CDS sometimes caused difficulty in determining the true cortical edge; this was especially a problem in thin bones, such as mandibles in the lateral position and vertebrae. Repeated cortical width measurements for each bone were compared using ANOVA. The results were similar to those achieved with the OGS; except for magnified alveolar bone height ($p < 0.001$) and mandibular standard inferior cortical width ($p < 0.005$), there were no significant differences when all measurements for a particular bone were compared.

Comparison of data using the manual (OGS and calipers) and computer digitizing systems

Optical grid and caliper results were compared with digitizing system results using paired t-tests. The results are shown in Table 3.2. There were significant differences ($p \leq 0.05$) between the manual and CDS results for every variable except for magnified medial cortical femoral width and standard lingual mandibular cortical width. For all variables except magnified medial femoral cortical width and the vertebral size, the values obtained using the digitizing system were larger than those obtained with manual methods.

For most variables, the mean coefficient of variation (CV%) for the CDS was the same or lower than for manual methods (OGS and calipers); for standard and magnified

inferior mandibular cortical width and magnified mandibular lingual cortical width, however, the OGS CV% were lower. Both of these cortices were difficult to measure and the larger CV% obtained in digitized images may have resulted from difficulty in locating the cortical edge during measurement. The CV% are shown in Table 3.1; values for manual methods and for the CDS ranged from 1% to 10% and 0.5% to 6% respectively.

Comparison of CV% obtained for standard vs. magnified views indicated that, in most cases the CV% obtained for magnified views was the same or lower than that for standard views. Exceptions to this trend were OGS buccal cortical width, CDS anterior femoral cortical width, and CDS anterior-posterior vertebral width, where the CV% for the magnified views were greater than for the standard views. In most cases, the CV% for the digital images were the same for both the standard and magnified views.

Accuracy of the Measurement Technique

The accuracy of the measurement technique and constancy of film quality, exposure and developing were determined by comparing measurements of radiographic images of a brass plate with direct measurements of the actual brass plate.

Analysis of the brass plate radiographic images

Analysis of the circle and interval widths indicated that there were no significant differences between measurements in the twenty images analyzed. The mean diameter of all circles was 0.961 mm and the mean width of all intervals was 1.006 mm.

Analysis of direct measurement of the brass plate

The mean diameter of the circles, measured on the actual brass plate, was 0.970 mm with a variance of 0.00172 whereas the mean width of the intervals was

1.03 mm with a variance of 0.0041. Comparison of the direct measurements of the brass plate with the measurements made on the radiographic images indicated that the accuracy of circle measurement was 0.93% and that of the interval measurement was 2.3%.

Animal Weights

Variability between matched treatment groups

Two rats in the 48 week-old BLC treatment group were obese at the time of sacrifice (821 and 799 g respectively) with an average weight of 540 g for the treatment group; these extreme values were identified as outliers by measures of skewness, kurtosis and normal probability plots, and deleted from the data set. After deleting extreme values, there were no significant differences between average weights of age-matched VND rats. Similar results were obtained for all BND and BLC rats. (Tables 3.3, 3.4, and 3.5).

Variability across treatment groups

No significant average weight differences were found across treatment groups for rats sacrificed at 18 and 24 weeks respectively ($p \leq 0.05$). For rats sacrificed at 36 weeks, the BLC treatment group was significantly heavier than the VND and BND rats at all times. There was no significant average weight difference between the VND and BND treatment groups for animals sacrificed at 36 weeks at any time. For rats sacrificed at 48 weeks, the BLC treatment group was significantly heavier than the VND and BND rats after 20 weeks. (Table 3.6 and Fig. 3.1).

Litter Size

Shortly after parturition, all litters were standardized to 12 pups, however, during the lactation period, not all pups in every litter survived. When the bred rats were sacrificed, litter size ranged from 0 to 12 pups with an average of 10-11 pups per litter. (Table 3.7) Analysis of the number of pups per litter for the BND and BLC treatment groups showed that there were no statistically significant differences ($p > 0.05$) between litter sizes.

Animal Sacrifice

Bone abnormalities

At sacrifice, morphological abnormalities were noted in two of the rats. One of the 24-week BLC rats had a grossly enlarged left femur which was widened in the medial-lateral plane and bowed in an anterior-posterior direction at the midshaft. During dissection, it was noted that soft tissue was more difficult to remove from the specimen. Radiographic examination revealed expanded but intact cortices with discontinuous remnants of the original cortices, bridged by new bone. The trabecular bone pattern of the femoral shaft was not homogenous. The radiographic impression was suggestive of a healed fracture which had not remodeled. Clinically, however, there was no evidence of a fracture, as would have been noted when the rat was weighed weekly, nor was there any sign of discomfort. Since longitudinal growth of the femur was not affected, the fracture must have occurred subsequent to the rapid growth phase in young rats, perhaps even prior to the study period, and was probably not due to the CDD. Histopathologic examination revealed bone marrow expansion with no neoplastic or abnormal bone evident with absence

of mitotic figures. This femur was not included in the study; the right femur was used instead.

One of the 24-week BND rats was noted clinically to have microphthalmia of the left eye. The head was retained for radiographic examination and it was found that the entire left side of the cranium, zygomatic arch complex and maxilla were also hypoplastic. This case was likely developmental in nature and not related to experimental conditions. For this animal, the right mandible was used for analysis.

During dissection of the BLC rats sacrificed at 18 and 24 weeks, the femurs were noted to have a different texture than those of the VND or BND treatment groups, feeling rough when scraped with the back of a scalpel blade during soft tissue removal. Gross examination revealed that the cortical bone was somewhat porous. This alteration was not seen in BLC rats sacrificed at ages 36 and 48 weeks, nor was it seen in any other treatment groups.

Subjective analysis of periodontal disease in the mandible

Periodontal bone loss was present in the mandibles of all rats, with greater severity of disease in BLC animals. In mild cases, only the first mandibular molar (M1) was affected, with exposure of the furcation on the lingual aspect. With increasing severity of bone loss, the lingual aspects of the roots of M1 were exposed, starting with the mesial root; the middle and distal roots were affected later. With further disease progression, the lingual aspects of the roots of the second (M2) and third (M3) molars were exposed. In all cases, M1 was the most severely-affected tooth and no bone loss occurred on the buccal aspects.

The VND rats had the mildest form of periodontal bone loss, usually affecting only the mesial root of M1. However, as the rats aged, as seen in animals sacrificed at 36 and 48 weeks, bone loss was more severe and spread to all roots of M1 and eventually to M2 and M3. Rats in the BND treatment group had a similar pattern of bone loss. The BLC

rats were similar to the VND animals until times 4 and 5, when periodontal bone loss in the BLC rats was more severe at M1 and also consistently affected M2 and M3.

No carious lesions were detected in any of the teeth examined, nor were any enamel defects or tooth fractures noted.

Bone Analysis

Precision of measurement

During the bone measurement phase of the study, a single set of three bones (mandible, femur and vertebra) was repeatedly measured to determine intra-observer error. Using ANOVA, there were no statistically significant differences between measurements of the same variable made 10 times over a period of 4 weeks. The results are shown in Tables 3.8, 3.9, and 3.10.

Difficulties encountered in data collection

In all cases, data acquisition was more difficult for BLC rats due to the skeletal osteopenia that developed. With the onset of osteopenia, radiographic contrast in all images was reduced and bony cortices did not appear as sharp as those in the normal diet groups.

Analysis of the femurs, mandibles and vertebrae indicated that measurement of cortical widths was more difficult in cases where bone was very thin, such as the mandible and vertebrae, and in specimens exhibiting osteopenia. Thin cortical plates gave faint radiographic images with poor contrast between bone and the black background. Adjusting brightness and contrast in the digitized images alleviated this problem somewhat but in several cases, images were still considered to be of suboptimal quality.

Femurs

All femoral cortices were well-defined in the radiographic images except for the medial cortex, where the endosteal surface was indistinct in some rats, causing some difficulty in locating the cortical edge.

Mandibles

Each hemi-mandible was very thin in the buccal-lingual plane so that only a relatively small volume of bone was available for analysis. In lateral views, the alveolar crest between the first and second molars was difficult to visualize in digitized images because it tapered sharply interproximally. Conversely, the inferior cortex was more radiopaque, but accurate measurements of its width were difficult because these were taken along the arc of a curve, along the line drawn over the pulp chamber of the first molar distal root.

Difficulty in measuring the width of the lingual cortex was encountered in occlusal views because the cortical plate of bone was thin, resulting in an ill-defined cortical edge. The buccal cortex was thicker due to bulkiness of the external oblique ridge, so its radiographic image was sharper.

Vertebrae

Because rat first lumbar vertebrae are composed of thin plates of bone, gross vertebral morphology was analyzed instead of cortical widths. However, locating the rostral and caudal cortical edges was difficult in lateral views because of poor radiographic contrast, necessitating drawing pencil lines on the film to outline these edges. Depending on the accuracy of tracing the edges, the accuracy of vertebral measurements were also affected.

Variation Over Time Within Treatment Groups

Each treatment group was analyzed separately to evaluate changes occurring over time. The 12-week baseline VND group was also compared to older BND and BLC animals to determine if any changes had occurred in these latter groups, compared with control animals.

Identification of extreme values

Although the numbers of rats in each study cell (n = 12) was small, the several individual measures made for each variable led us to believe that all variables would have an approximate normal probability distribution. This assumption was tested by measures of kurtosis, skewness and normal probability plots. Outliers identified in this process were reviewed, and if no methodological error could be found, were eliminated from the analysis.

The Bartlett test indicated that for several variables in the femurs, mandibles and vertebrae, variances were not homogenous in each of the treatment groups of animals at every measurement period. These inconsistencies were due in part to measurement variability and also to individual animal variations. For the purposes of an overall analysis, these few inconsistencies were disregarded.

Femurs

The femoral cortical width measurements are summarized in Table 3.11. For all cortical widths, in both standard and magnified views, the VND treatment group at 12 vs. 18 and later at 36 vs. 48 weeks were not statistically different, however, femoral cortical widths at 12 and 18 vs. 24, 36 and 48 weeks, as well as at 24 vs. 36 and 48 weeks, were significantly different ($p \leq 0.05$). (Plates 1, 2, 3, and 4.) The only exceptions were magnified views of posterior cortical width, where VND rats at 12 vs. 18 weeks were also

different from each other. The cortical width at 18 weeks is more than three standard deviations larger than the value at 12 weeks and was therefore eliminated from the analysis. There were no differences in cortical widths at 36 vs. 48 weeks. Variances for measures of standard and magnified posterior cortical width, magnified anterior cortical width, and magnified lateral cortical width for VND animals were not homogenous (Bartlett test); comparisons between these measures were therefore made using the Kruskal-Wallis test.

For standard and magnified total femoral width in the anterior-posterior plane, there were no differences between VND rats at 12 vs. 18 or 18 vs. 24 weeks. However, there were statistically significant differences at 12 vs. 18 vs. 24, 36 and 48 weeks and at 24 vs. 36 and 48 weeks but no differences at 36 vs. 48 weeks. (Fig. 3.2)

For standard total femoral width in the lateral plane, the only significant differences were between rats at 36 and 48 weeks vs. those at 12 and 18 weeks. Similar results were obtained in the magnified views except additional significant differences were found between rats at 12 vs. 24 weeks and 24 vs. 48 weeks but no difference at 24 vs. 36 weeks.

For the BND treatment group, no difference was found for femur variables between VND rats at 12 weeks (ie. control baseline) vs. BND rats at 18 weeks, except for magnified posterior cortical width, which was significantly different (more than two standard deviations higher) in BND rats. For measures of standard and magnified anterior cortical width, standard posterior cortical width, magnified total lateral width, standard and magnified medial cortical width, standard and magnified total A-P width, measures for 12-week VND rats and 18-week BND rats differed from those of older BND rats at 24, 36, and 48 weeks. However, there were no differences in the BND rats at 24 vs. 36 and 48 weeks, and at 36 vs. 48 weeks. Similar results were obtained for the remaining variables with the following exceptions: for standard total lateral width, there was no difference at 18 vs. 24 weeks; for standard lateral cortical width, there was a significant difference at 24 vs. 36 and 48 weeks; and for magnified lateral cortical width, there was a significant

difference at 24 vs. 48 weeks. The values for these variables at 24 weeks were two standard deviations lower than those at later times and therefore represent outliers.

For BND rats, the Bartlett test indicated that variances for measures of standard and magnified anterior cortical width, magnified posterior cortical width, standard lateral cortical width and magnified medial cortical width were not homogenous, and the Krushkal-Wallis test used for comparisons of these variables.

For the BLC treatment group, the following femoral cortical widths at 18 weeks were significantly different from those measured at any other time: standard and magnified anterior, posterior, lateral and medial cortical widths. (Fig. 3.3) Similar results were obtained for the remaining femur variables with the following exceptions: for standard and magnified total lateral width, there was no difference between 12-week VND rats vs. 18-week BLC rats. There were also no differences in the BLC group at 24 vs. 36 and 36 vs. 48 weeks but significant differences at all other times. For magnified anterior and posterior cortical widths, there were additional significant differences between 12-week BND rats vs. 36-week BLC rats. For standard lateral cortical width, there was a difference at 24 vs. 36 weeks but not at 24 vs. 48 or 36 vs. 48 weeks. For standard total A-P width, measures for 12-week VND rats and 18-week BLC rats were different from BLC rats at all other ages and different from each other. There was also a significant difference in values obtained at 24 vs. 36 weeks. Similar results were obtained for magnified total A-P width except that there was no difference at 24 vs. 36 weeks.

For BLC rats, the Bartlett test indicated that variances for standard and magnified anterior and posterior cortical width were not homogenous, and the Krushkal-Wallis test used for comparisons of these variables.

Mandibles

The data for mandibular cortical width measurements are summarized in Table 3.12 and Fig 3.4. No significant differences were found between VND rats for all variables

measured in the mandible except for the following: for standard buccal cortical width, animals at 12 weeks were significantly different from those at 18, 36 and 48 weeks but not at 24 weeks. Similar results were obtained for magnified buccal cortical width except that there was a difference at 12 vs. 24 weeks. The mean values for the 12-week rats were one to two standard deviations below those for the older VND rats and likely represented outliers, since later in the analysis of the BND group, there were no differences between 12-week VND rats and 18-week BND rats. For magnified total mandibular width, the only significant differences were at 12 and 18 vs. 36 and 48 weeks.

The Bartlett test indicated that variances for standard and magnified inferior and buccal cortical widths and magnified total mandibular width were not homogenous in the VND treatment group, and the Krushkal-Wallis test was used for comparisons of these variables.

For the BND treatment group, no differences were found over time except for measurements of standard inferior cortical width and standard and magnified alveolar bone height. For standard inferior cortical width, a significant difference was found at 36 vs. 48 weeks, however, the mean value at 48 weeks was only one standard deviation lower than that obtained at 36 weeks, so the apparent difference was not very great. Furthermore, there was no difference between standard and magnified views for the rats at 36 vs. 48 weeks. For standard alveolar bone height, significant differences were found when 12-week VND rats and 18-week BND rats were compared to BND rats at 36 and 48 weeks. Additional differences were found between BND rats at 24 vs. 48 weeks. For magnified alveolar bone height, significant differences were found between 12-week BND rats vs. 24, 36 and 48-week BND rats, with additional differences at 18 vs. 36 and 48 weeks. The values for 12-week VND and 18-week BND rats were one to two standard deviations below those for older animals. These apparent differences in younger animals may have been due to measurement inconsistencies because of difficulty in visualizing the crestal cortex in digitized images.

Comparison of measures of mandibular variab[illegible] BLC treatment group indicated that there were significant differences between rats a[illegible] and 48 weeks cor[illegible]d with earlier measurements for measures of standard and magnified buccal cortical width and magnified total mandibular width. In addition, measures at 36 vs. 48 weeks differed for standard buccal cortical width but were similar for magnified buccal cortical width and magnified total width. For standard and magnified inferior cortical width measurements, the only significant difference was at 18 vs. 48 weeks. For standard alveolar bone height, significant differences were found between VND rats at 12 weeks vs. BLC rats at 48 weeks and BLC rats at 24 vs. 48 weeks. Similar results were obtained for magnified views but with a significant difference also occurring at 18 vs. 48 weeks. For standard lingual cortical width, only VND rats at 12 weeks were significantly different from older BLC rats whereas there were no differences between 12-week VND or older BLC rats in the magnified views. The lingual cortex remained unchanged over time in BLC rats. For measures of total mandibular width, significant differences were found at 18 vs. 36 and 48 weeks; and at 24 vs. 36 weeks in standard views. In magnified views, no difference was found at 36 vs. 48 weeks but rats at 36 and 48 weeks differed from younger animals.

The Bartlett test indicated that measures of magnified inferior cortical width and standard lingual cortical width did not have homogeneity of variance, and the Krushkal-Wallis test was used for comparisons of these variables.

Vertebrae

Vertebral measurements are summarized in Table 3.13 and Fig. 3.5. Vertebral images were difficult to measure because the bony plates were very thin, resulting in indistinct digitized images and loss of measurement accuracy, reflected by inconsistencies in the data. The random nature of the significant differences is more consistent with difficulty in obtaining consistent measurements than with true vertebral changes.

Analysis for vertebral measures in the VND treatment group indicated that for standard A-P width and standard and magnified midbody height, significant differences were found at 12 and 18 vs. 48 weeks. For standard and magnified anterior height, significant differences were found at 12, 18, and 24 vs. 48 weeks. For magnified A-P width, the only significant difference found was at 18 vs. 48 weeks.

For the BND treatment group, generally, only the VND treatment group at 12 weeks differed from the BND treatment group at most ages. For standard A-P width, magnified anterior height and magnified midbody height, there was no significant difference between the baseline VND group at 12 weeks vs. BND rats at 18 weeks but a significant difference between 12-week VND rats vs. BND rats at 24, 36 and 48 weeks. For standard anterior height and standard midbody height, VND rats at 12 weeks differed from BND rats of all other ages. For magnified A-P width, the only significant difference was between baseline VND rats vs. 48-week BND rats.

For for all vertebral measures in the BLC treatment group, the baseline VND treatment group at 12 weeks differed from BLC rats by age 24 weeks for standard and magnified A-P width and standard anterior height; and by age 36 weeks for standard and magnified midbody height, and magnified anterior height. For standard anterior-posterior width, animals at 18 weeks were different from those at 24 and 36 weeks but were similar to those at 48 weeks. VND rats at 12 weeks differed from 24, 36 and 48-week BLC rats. There were no differences for BLC rats at 24 vs. 36 and 48 weeks; and at 36 vs. 48 weeks for standard A-P width. However, for magnified anterior-posterior width, rats at 18 weeks differed from those at 36 and 48 weeks and there were also differences between 12-week VND vs. 24, 36 and 48-week BLC rats. For measures of standard anterior vertebral height, BLC rats at 18 weeks differed from those at 36 and 48 weeks and rats at 24 weeks differed from those at 48 weeks, with no differences at 24 vs. 36 weeks. Similar results were obtained for magnified views with additional differences between 12-week VND rats vs. 36 and 48-week BLC rats. For measures of standard midbody height, BLC rats at 18

and 24 weeks differed from those at 48 weeks and 12-week VND rats differed from BLC rats at 36 and 48 weeks. Similar results were obtained for the magnified views except that there was also a difference between BLC rats aged 18 and 24 vs. 36 weeks.

The Bartlett test for homogeneity of variance indicated that except for standard anterior-posterior vertebral width in the BLC rats, all vertebral measures for all treatment groups had homogenous variances.

In a multivariate analysis of covariance for each treatment group over time (ie. at different ages), weight and age contributed significantly to the variance in some measured variables.

Variation Over Time Across Treatment Groups

Measurements for mandibles, femurs and vertebrae were compared between treatment groups at each time during the experiment. Animals aged 12 weeks were excluded from this analysis because this group consisted of only one treatment group, ie. a VND group.

Femurs

A comparison of femoral cortical width measurements between treatment groups using ANOVA with significance determined using a Tukey HSD test, is summarized in Table 3.14. At 18 weeks, the BLC treatment group differed from VND and BND rats for standard and magnified measures of anterior, posterior, lateral and medial cortical widths. No significant difference was found between treatment groups for standard and magnified measures of total lateral and anterior-posterior widths.